Title:

Functional morphology of the tongue and laryngeal entrance and scanning electron microscopic pattern of the filter feeding apparatus of *Anas crecca*

Authors and affiliations:

Reem S. Alruhaimi[1], Mohamed M. A. Abumandour[2]*, Mohammed Kassab[3], Ahmed Elnegiry[4], Foad Farrag[5], Diaa Massoud[6], Ayman M. Mahmoud[7, 8], Bandar H. AL-Osaimi[9], Hazem Hamoda[10]

1. Department of Biology, College of Science, Princess Nourah bint Abdulrahman University, Riyadh 11671, Saudi Arabia.
2. Department of Anatomy and Embryology, Faculty of Veterinary Medicine, Alexandria University, Alexandria, Egypt.
3. Department of Cytology and Histology, Faculty of Veterinary Medicine, Kafrelsheikh University, Kafrelsheikh, Egypt.
4. Department of Histology and Cytology, Faculty of Veterinary Medicine, Aswan University, Aswan, Egypt.
5. Department of Anatomy and Embryology, Faculty of Veterinary Medicine, Kafrelsheikh University, 33511 Kafrelsheikh, Egypt.
6. Department of Biology, College of Science, Jouf University, Sakaka, Saudi Arabia.
7. Department of Life Sciences, Faculty of Science and Engineering, Manchester Metropolitan University, Manchester, UK.
8. Molecular Physiology Division, Zoology Department, Faculty of Science, Beni-Suef University, Beni-Suef, Egypt.
9. Department of Zoology, College of Science, King Saud University, Riyadh 11451, Saudi Arabia.
10. Department of Anatomy and Embryology, Faculty of Veterinary Medicine, Aswan University, Aswan, Egypt.

Corresponding author: ***Mohamed Abumandour,*** Professor of Anatomy and Embryology, Faculty of Veterinary Medicine, Alexandria University, Alexandria 21944, Egypt.

The mailing address of the corresponding author: Department of Anatomy and Embryology, Faculty of Veterinary Medicine, Alexandria University, Abees 10th, Alexandria 21944, Egypt. Tel.: +201000322937; Fax: +20452960450.

ORCID ID of the corresponding author: 0000-0002-3289-1982

E-Mail address of the corresponding author: m.abumandour@yahoo.com or M.abumandour@alexu.edu.eg

ABSTRACT

There is insufficient information about the migratory Eurasian teal, *Anas crecca*. The study provides the first anatomical description of lingual adaptations and their relationship with the species-specific feeding behavior of *Anas crecca* collected near Egyptian Lake Nasser. Our investigation was applied with the help of gross, scanning electron microscopy (SEM), and morphometric analysis. The study focused on the feeding filtering apparatus that depends on eight lingual papillae. The spatula-shaped nail is adapted for food particle pecking, while the lingual combs, rostral border of the prominence, unique papillary crest, median groove, and papillary system aid in intra-oral transportation. The feeding apparatus is formed by the lateral and dorsal papillary systems. The lateral papillary system had conical papillae with numerous long filiform and hair-like filiform papillae to constitute the food filtration apparatus, while the dorsal papillary system had ridged-like and rod-like papillae in addition to the small papillae of the papillary crest and spinated border of the root to help in moving the food particles with water to the lateral sides of the prominence. The laryngeal region exhibited papillary (pre-glottic) and non-papillary (glottic) areas. The papillary area had two lateral papillary portions and a median smooth portion, while the non-papillary area had an ovoid laryngeal mound with a median glottic opening that was bordered by a papillary border. The papillary portion had three slightly oblique longitudinal papillary rows.

Keywords**:** *Anas crecca*; Filter feeding apparatus; Laryngeal mound; Lingual comb; Lingual papillae.

1- Introduction

Anas crecca, also known as the Eurasian teal, common teal, or Eurasian green-winged teal, is a common migratory waterbird duck that breeds in Asia and Europe before migrating to the Mediterranean during winter. The Nile Valley, particularly Lake Nasser, is a significant wintering destination, according to BirdLife International (2020). *A. crecca*, a species in the *Anas* genus, belongs to the *Anatidae* family and is covered under the Agreement on the Conservation of African-Eurasian Migratory Waterfowl (AEWA). In the spring and summer, *A. crecca primarily* feeds on mollusks, worms, insects, and crabs, occasionally diving for prey while submerging its head, and typically consumes through dabbing, upending, or grazing (Madge & Burn, 1988). In winter, it adopts a granivorous diet, consuming grass seeds and aquatic plants like sedges and grains. During the breeding season, despite winter nocturnal habits, diurnal feeding habits are present.

The feeding process in vertebrates involves ingestion, intra-oral transport, and swallowing, with evolutionary differences between neognathous and paleognathous bird groups identified through behavioral analysis (Schwenk & Rubega, 2005; Tomlinson, 2000). Paleognathous birds adopt a cranioinertial mechanism, where food is directly transported into the esophagus without using the tongue. The beak and hyolingual apparatus's intricate movements are linked to the lingual feeding mechanism utilized by neognathous birds. Neognathous birds occasionally employ a catch-and-throw system for swallowing large food particles, requiring intricate movements of the hyolingual apparatus. Toucans, hornbills, and southern cassowaries are outliers in neognathous birds due to their development of ballistic transport (Baussart & Bels, 2011; Bels & Baussart, 2006). Wild ducks have the ability to pick up and toss grains smaller than a pea, remove grass blades, and maintain their ability to do so (Kooloos et al., 1989).

Wild ducks use a filter-feeding strategy to consume food submerged in water, as per various studies (Abumandour et al., 2019; Kooloos et al., 1989; Tomlinson, 2000). Filtration demonstrates typical neognathous bird behaviors, such as ducks using lingual feeding and under-tongue conveyance (Kooloos et al., 1989; Tomlinson, 2000). Most published articles focus on the anatomical description of the tongue of avian species other than the Anatidae family, with little attention given to the study of the laryngeal mound and its role in food particle movement (Abumandour, El-Bakary, et al., 2021; Abumandour, Farrag, et al., 2021; Bassuoni et al., 2022; El-Mansi et al., 2020; El-Mansi et al., 2021; Gewaily & Abumandour, 2020). Published data on the tongue of certain *Anatidae* family birds has been found to completely ignore the laryngeal mound (Abumandour et al., 2019; Jackowiak et al., 2011; Skieresz-Szewczyk & Jackowiak, 2014; Skieresz-Szewczyk & Jackowiak, 2016; Skieresz-Szewczyk et al., 2014; Skieresz-Szewczyk et al., 2014; Tawfiek & Mahmoud, 2020). The previous published data indicated that a bird's tongue's structural properties can adapt to its eating habits, providing insight into its environment and lifestyle (Gewaily & Abumandour, 2020). Ostrich and Eurasian hoopoe tongues are adapted for swallowing and moving food particles (Abumandour & Gewaily, 2019b; Tadjalli et al., 2008), while piscivorous species like penguins have stiff, pointed, caudally oriented lingual papillae that are specialized for gripping and handling food, allowing them to retain slippery prey (Abumandour et al., 2019).

Meanwhile, the elongated tongue of grain-, insectivore-, and carnivore-feeding species allows for selective, rejecting, accepting, catching, and manipulating feeding materials (Abumandour, Farrag, et al., 2021; El-Mansi et al., 2020; El-Mansi et al., 2021).

The morphological characteristics of the tongue and laryngeal mound of the Eurasian Teal *A. crecca* are insufficiently understood, with limited information available on their role in feeding mechanisms. Therefore, our study utilized gross and scanning electron microscopic (SEM) examinations to study the structural adaptations of the tongue and laryngeal mound in the feeding filtering apparatus of migratory Eurasian Teal *A. crecca* collected around Lake Nasser in Egypt. Then, the findings are compared to existing published information on various avian species.

2. Materials and Methods

2.1. Collection of samples and gross anatomical examination

This study was carried out according to the Institutional Animal Care and Use Committee (IACUC) protocols of Laboratory Animals, Faculty of Veterinary Medicine, Alexandria University (Approval No.: 11/3/2023/231). Ten Eurasian Teal (*A. crecca*) duck weighting averages of 2.73 kg were obtained from a local hunter near Lake Nasser in Aswan (Egypt). The collected ducks were kept in the animal housing following the guidelines established for the 'Sampling protocol for the pilot collection of catch, effort, and biological data in Egypt' (Dimech et al., 2012). The *Anas crecca* included in the study had no oropharyngeal anatomical abnormalities. The *Anas crecca* were anesthetized with pentobarbitone sodium administered through the internal carotid artery with warm physiological saline (35 °C). The tongues and laryngeal mounds obtained by dissecting the oropharyngeal cavity longitudinally (n = 5) were examined grossly to determine their morphological and morphometric features and were photographed on five samples using a digital camera (*Canon IXY 325, Japan*). The anatomical terminology was used according to Baumel et al (1993).

2.2. SEM examinations

To study the ultrastructure characterizations five samples were used from the different lingual parts (apex, body, lingual prominence, root) and the two parts of the laryngeal entrance, according to (Abumandour et al., 2024); Alruhaimi et al. (2024). The samples were fixed at 4 °C in 2% formaldehyde and 1.25% glutaraldehyde in a 0.1 M sodium cacodylate buffer (pH 7.2). The samples were washed in 0.1 M sodium cacodylate containing 5% sucrose, processed through tannic acid, and finally dehydrated in increasing concentrations of ethanol (50, 70, 80, 90, 95, and 100% ethanol, 15 min each). After critical point drying in carbon dioxide, the samples were attached to stubs with colloidal carbon and coated with gold palladium in a sputtering device (Elghoul et al., 2022; Kandyle et al., 2022; Massoud et al., 2023). Specimens were examined and photographed with a JEOL SEM operating at 15 KV at the Faculty of Science, Alexandria University, Egypt.

2.3. Digital coloring of scanning electron microscopic images

We digitally colored the SEM images using the Photo Filter 6.3.2 program to identify the various structures. This technique was previously described by (Abumandour et al., 2023); Kandyel et al. (2023); Roshdy et al. (2021).

2.4. Gross and SEM Morphometric Analysis

The different dimensions of tongue with its parts and laryngeal mound with its parts were measured using an electronic ruler with an accuracy of 0.1 mm (Abumandour & Hanafy, 2024; Kandyel, El Basyouny, Albogami, et al., 2024; Kandyel, El Basyouny, El-Nagar, et al., 2024). The obtained SEM images were processed by the ImageJ software to determine the different measurements of the tongue and its anatomical structures (Schneider et al., 2012). Then, the data were presented as the mean ± standard error (SE).

3. Results

The filter-feeding apparatus of the migratory *Anas crecca* is primarily formed from the tongue and its papillary system. The floor of the oropharyngeal cavity consisted of the tongue and laryngeal entrance, as depicted in various figures (Figs. 1A, 2A, and 5A).

3.1. Tongue

3.1. 1. Gross Morphometric Analysis

The tongue consists of the free rostral and fixed caudal parts. The rostral lingual part represented 67% and the caudal part 33% of the tongue length (Table 1). The lingual nail represented 9.5%, the apex 33%, the body 57%, and the root 9.5% of the tongue length (Table 1). The body is the widest and thickest part (0.85 ± 0.32 cm and 0.5 ± 0.1 cm, respectively), while the lingual nail is the narrowest and least thickest part (0.6 ± 0.10 cm and 0.2 ± 0.01 cm, respectively), as shown in (Table 1). The lingual groove was represented by 33%, the lateral serrated border of the root 6%, the papillary crest 33%, and each half part of the dorsal spinated border of the root 7% of the tongue length (Table 1). The papillary triangular area represented 30%, and the non-papillary glottic elevated area (Laryngeal mound) represented 70% of the pharyngeal cavity length (Table 2). The equatorial diameter of the laryngeal mound reached 2.8 ± 0.54 cm, while the axial diameter of the laryngeal mound reached 1.52 ± 0.64 cm (Table 2). The glottic opening represented about 38% of the pharyngeal length. The laryngeal mound had different widths, reaching 0.45 ± 0.12 cm at its rostral part, 0.61 ± 0.24 cm at its middle part, and 0.3 ± 0.11 cm at its caudal part (Table 2).

3.1. 2. Gross observations

Grossly, the oropharyngeal cavity floor enclosed the elongated, flattened, non-protrusible tongue, which was fixed inside the deep sublingual space by a lingual frenulum at its caudal part, just at the level of the lingual prominence (Figs. 1A, 1D, 3H/LF and SLS). The three lingual areas were the apex, body, and root (Fig. 1A–D/AP, LB, and LR). The lingual groove was clear and extended from the rostral border of the lingual nail to the papillary crest, in which it was shallow on the nail and lingual prominence but deep on the apex and deepest on the body (Figs. 1A-B, 2A, 3A, 4A, 5A, 6A, 7A, and 9A/LG).

The lingual apex consists of a round anterior spatula-like portion (lingual nail) and a caudal portion, separated by a short lateral transverse fissure (Figs. 1B-C, 2A, 3A, 4A, 5A/LA, LT, LN, AC, TG). It carried numerous papillae on its dorsal and lateral surfaces, except for the nail (Figs. 1B, 2A, 3A, 4A, 5A/AC, HP). The lingual body consisted of two regions: the rostral pyramidal region and the caudal elevated triangular lingual prominence (Fig. 1A/LB, BP, LP). The rostral pyramidal region carried the lingual comb on its dorsal surface and numerous papillae on its lateral surface (Figs. 1A-C, 2A, 3A, 3H, 4A, 5A, 6A, 7A, 9A/PYS, LB, BP, LP, SCP), while the lingual prominence carried conical papillae and filiform papillae on its rostral part, while its caudal part of the lateral portion carried some filiform papillae and a lateral serrated border (Fig. 1B/LP, LCPT, red star, PFP, PB).

The short lingual root consisted of two portions (right and left) separated by a narrow space, and it is surrounded by spinated borders from all directions. It is separated rostrally from the lingual prominence by the papillary crest and laterally by a lateral serrated border, and it is separated caudally from the laryngeal entrance by the dorsal serrated border, which consists of two portions (right and left) separated by a narrow space (Figs. 1A, 7A, 8A, 9A, and 10A-B/LR, PB, SB, PC, and blue arrowheads).

3.1. 3. Scanning electron microscopic observations

The anterior spatula (cranial portion of apex) had a round apex and was demarcated laterally from the rest of the apex by a short lateral transverse fissure (Figs. 1E, 2B/LN, TG), and its dorsal surface had a shallow median longitudinal lingual groove. High SEM magnification revealed numerous small tubercles in the median area, folds in the peripheral area, and various shapes of micro-cells surrounded by micro-grooves on the ventral surface (Fig. 1E-H/DLS, VLS, LN, LG, AF, MC, green stars, and arrowheads). The dorsal surface of the caudal portion of the apex was divided into two wide lateral regions by a deep part of the median lingual groove. The dorsal surface exhibited numerous ridge-like papillae with a projected base (at its origin near the groove) and small pointed filiform papillae in the lateral regions (Figs. 2C-D, 3B-J/RPP, HS, SFP). High SEM magnification revealed ridge-like triangular papillae with a pointed apex, dorsal border, and a wide base attached to the dorsal lingual surface, which was surrounded by numerous scales (Figs. 2D and 3D-F/RPP, BS).

The pyramidal region consisted of two parts: small rostral and large caudal parts. The small rostral part, located rostral to the lingual comb, had numerous rod-like filiform papillae with a projected base, small conical papillae on its lateral regions of the dorsal surface, and numerous ventral rod-like filiform papillae on its lateral border (Figs. 4B-D, 8B-C/RFP, PS, SCP, and RFPV). Meanwhile, the lingual comb in the large caudal part had randomly distributed spines, round and elongated tubercles, small filiform papillae, and lingual salivary gland openings. Its lateral border had large quadrilateral conical papillae rostrally and large triangular conical papillae with numerous hair-like filiform papillae caudally just at the level of the head and caudal part of the lingual comb (Figs. 5B-F/RFP, PS, RS, RB, RT, ET, LCPQ, LCPT, and red arrowheads). High SEM magnification revealed one to three ridges on the dorsal surface of the quadrilateral large conical papillae (Fig. 8B-C/LCPQ, red stars).

The pyramidal lingual comb consisted of two halves separated by a shallow lingual groove, as shown in (Figs. 5B-F, 6B-C/PYS, He, Cd, Cr, Rr, and LG). Each half of the comb had two regions that named from caudal to rostral as the followings; the smooth head and long thread-like regions that was subdivided into three parts according its appearance; the first smooth caudal part that joined to the pyramidal head, while the middle serrated part had about 14-15 laterally directed triangular processes, but the rostral part was consisted of three laterally serrated tubercles; the large caudal serrated tubercle had 7-8 laterally directed processes, the middle serrated one had 5-6 laterally directed processes, and the small ovoid rostral tubercle had only one or two laterally directed processes (Figs. 5B-F, 6B-C, 6F/PYS, He, Cd, Cr, Rr, red, green, blue arrowheads).

The rostral ¾ part of the dorsal surface of lingual prominence was divided into parts by a shallow lingual groove, while its caudal ¼ part was devoid of this groove (Figs. 6B-F, 7B-D/LP, LG). The lingual prominence's lateral surface had a serrated border of 10–12 triangular-pointed processes rostrally and a wedge-shaped structure caudally, as shown in (Figs. 6B-F, 7B-D/LP, red stars, LW). The lateral border of the lingual prominence carried the large triangular conical papillae, hair-like filiform papillae, and ventral rod-like filiform papillae rostrally just adjacent to its lateral serrated border (Figs. 6B, 6F, 7B, 8D-E/LCPT, HFP, RFPV, red stars), while caudally, it had numerous small pointed filiform papillae adjacent to the wedged-shape structure (Fig. 10B-E/PFP, LW). High SEM magnifications revealed numerous scales and ridges on conical papillae, with large triangular papillae having an accessory wing-like structure (Figs. 7C-D, 8D-E/LS, red stars, AC).

The lingual prominence and root were separated by the semilunar caudally curved papillary crest with its caudally oriented mechanically conical papillae, with the complete absence of the giant laterally situated conical papillae. The papillary crest consisted of two transverse papillary rows; the dorsal row had 16–18 large triangular papillae, in which each of the three median papillae carried small accessory papillae with numerous scales, and the ventral row had 14–16 small conical-pointed papillae, in which the median two were fused together (Figs. 7E-G/PC, PCD, red arrowheads, PCV, white *).

The short lingual root is bounded by spinated borders on all sides, including the papillary crest rostrally, the lateral serrated border laterally, and the dorsal spinated border caudally, which consisted of two halves (right and left) by a narrow median passway, leaving the small smooth semilunar area of the root (Figs. 7E-F, 9C-E/LR, MLR, PC, SB, PB, blue arrowheads). A narrow, smooth median passway of the root was communicated between the small, smooth semilunar area of the root and the rostral part of the laryngeal entrance, and it was separated from the medial border of each spinated area bordered by the elevated longitudinal ridge on each side (Fig. 9C-E/green arrowheads).

The dorsal spinated border measured 0.4 ± 0.1 cm in width and 0.4 ± 0.02 cm in length for each half, respectively. This border was divided into two halves (right and left) by a median passageway; each half had two papillary rows; the dorsal row had 7-8 small pointed conical papillae, and the ventral row had 6-7 large triangular pointed conical papillae (Fig.

9C-F/SBR, SBP). High magnification revealed numerous small scales on the papillary surface (Fig. 9F/SBR, SBP). The lateral serrated border of the root measured 0.25 ± 0.01 cm in width and 0.4 ± 0.03 cm in length and carried 10–11 pointed triangular papillae on its free lateral border (Fig. 7B, 7E-G/PB). High magnification revealed numerous small scales on this lateral border (Fig. 7G/PB).

The median lingual groove extended along the lingual apex and body, including the nail, except for the caudal ¼ part of the lingual prominence that was devoid of this groove (Figs. 1E, 2C-E, 3B-C, 3G, 4B-E/LG, MG). The groove on the lingual nail and prominence was a shallow groove, but it appears deep on the apex and body (Figs. 1E, 7B, 7F/LG, MG). The groove on the apex and rostral part of the body had a triangular shape and is divided into two halves by a single deep median groove of the same width along the apex, while the main lingual groove began narrow rostrally and gradually increased in width caudally (Figs. 2C-E, 3B-C, 3G, 4B-E/LG, MG). Moreover, this groove appears as a single deep groove between the two parts of the lingual comb (Figs. 5B-F, 6B-C, and 6F/LG).

3.1. 4. Scanning electron microscopic observations

The longest and widest lingual papillary type was the large quadrilateral conical papillary type, while the shortest was the hair-like filiform papillae, and the narrowest was the hair-like filiform papillae. In the apex, the ridge-like papillary type had the longest papillae (1.7 ± 0.53), and the widest was the small pointed filiform papillary type (0.39 ± 0.12), as shown in (Table 3). In the lingual body, the large quadrilateral conical papillary type had the longest papillae (2.5 ± 0.78), followed by the ventral rod-like filiform papillae (2.13 ± 0.47) and the large triangular conical papillae, while the shortest was the hair-like filiform papillae (0.31 ± 0.02). The widest type was the large quadrilateral conical papillary type (0.89 ± 0.34), then the large triangular conical papillae (0.51 ± 0.1), while the narrowest was the hair-like filiform papillae (0.032 ± 0.01), as shown in (Table 3). In the papillary crest, the longest and widest papillae were observed on the dorsal papillary row. In the dorsal spinated border of the root, the longest (0.45 ± 0.02) and widest (0.17 ± 0.02) papillae were the large triangular pointed conical papillae of the ventral row (Table 4).

3.2. The laryngeal region

3.2. 1. Gross observations

The laryngeal region was separated from the lingual root by the dorsal spinated border, and it was bordered laterally by the longitudinal papillary row (Figs. 1A, 7A, 9A-B, 10A/LR, PR, HB). The laryngeal region was divided into two areas: the papillary (pre-glottic) triangular area and the non-papillary (glottic) elevated area (Figs. 1A, 7A, 9A-B, 10A/PTA, NER). The papillary area was bordered by a narrow median smooth passway and a dorsal spinated border rostrally, by the non-papillary area caudally, and by its lateral papillary row laterally (Figs. 9B, 10A/PTA, HP, and HPL). The apex of the papillary region was directed rostrally just at a narrow median smooth passway and had numerous papillae that were arranged in three rows (Figs. 9A, 10A/PTA, HP, HPM, HPE, and HPL). The non-papillary area is represented by the elevated ovoid laryngeal mound (*Mons laryngealis*) with a median longitudinal opening called the laryngeal cleft (glottis), bordered by the papillary border. The glottis communicates the pharyngeal cavity to the trachea and continues as a laryngeal fissure (Figs. 9A, 10A/GO, white and blue arrowheads, and LF). The non-papillary area is surrounded caudally by diamond-shaped pharyngeal conical papillae, indicating the laryngeal mound from the esophagus (Figs. 9A, 10A/PP, ES).

3.2. 2. Scanning electron microscopic observations

The laryngeal region was bordered laterally by the longitudinally elevated ridge of 18–20 small caudally directed papillae (Fig. 10B–C, 10E/HB, green arrowheads). The papillary triangular area had three portions: two lateral papillary portions of the caudolaterally directed papillae and the median smooth portion. The lateral papillary portion had three slightly oblique longitudinal papillary rows (lateral, middle, and medial), in which the lateral papillary row had 6-7 large, long pointed conical papillae with 4-5 small accessory conical papillae in-between (Fig. 9C-G/HPL, red stars), the middle one had 6-8 conical papillae with 6-7 small accessory conical papillae in-between (Fig. 9C-G/HPM, green stars), and the medial row had 4-5 triangular pointed papillae and was located just lateral to the rostral portion of the lateral border of the glottic opening (Fig. 9C-G/HPE, GO). The median smooth portion was located just opposite the median passageway of the lingual root rostrally and the rostral beginning of the glottic opening caudally; additionally, this portion had a small number of the laryngeal salivary glands (Fig. 9C-E/MPA, yellow arrowheads). High magnification revealed numerous small scales on the papillary surface (Fig. 9G/HS).

The non-papillary area had an elevated ovoid laryngeal mound with its median glottis (Figs. 9C, 10B/NER, LM, GO, LF). This area was bordered by the medial papillary row of the non-papillary area at its rostral portion and caudally by the diamond-shape pharyngeal papillae with numerous caudally directed mechanical conical papillae (Figs. 9C-D, 10B/NER, HPE, PP). The laryngeal mound was divided into two plates (right and left) by the median longitudinal glottic opening that was bordered by a slightly elevated papillary border of 10–12 caudomedially directed conical papillae; these papillae began small rostrally and increased in size caudally (Fig. 10B-C, 10E/LM, GO, GB, blue arrowheads). The glottis was continued caudally as a laryngeal fissure that was bordered by 2-4 small papillae on each side (Fig. 10B-C, 10E/LF, white arrowheads) at its rostral portion before beginning the pharyngeal papillae, while the rest of the fissure was bordered by the longitudinal pharyngeal papillary row of the large caudally directed conical papillae (Fig. 10E-F/GPL). High magnification revealed that each plate of the laryngeal mound was devoid of any papillae with a small number of laryngeal salivary gland openings (Fig. 10C–D/red arrowheads).

The diamond-shaped pharyngeal papillae were arranged in 7 or 8 overlapped transverse rows and one longitudinal papillary row of the caudally directed mechanical papillae (Fig. 10E-F/PP). The rostral row had 8–9 longest triangular-pointed papillae (Fig. 10E–F/GPT), and then decreased gradually on the rest of the transverse papillary rows to 2-3 small papillae on the most caudal (last) row (Fig. 10E–F/SP, SP1–7). The longitudinal papillary row had 5–6 long, pointed papillae (Fig. 10E–F/GPL). High magnification revealed numerous small scales on the papillary surface (Fig. 10F).

3.2. 3. Scanning electron microscopic Morphometric analysis of the tongue

In the lateral papillary portion of the triangular laryngeal area, the longest and widest papillary type is the large pointed conical papillae that formed the lateral longitudinal row, then the triangular pointed papillae that formed the medial longitudinal row, and the shortest and narrowest ones are the small accessory papillae that formed the middle longitudinal row, and then the small accessory papillae that formed the lateral longitudinal row (Table 5).

4. Discussion

This study represents the first gross and SEM depictions of the tongue and laryngeal entrance of the migratory Eurasian teal, with unique insight into its filter feeding apparatus and the influence of dietary habits, readily available nutrient components, and environmental, migratory, and climatic factors on their morphological adaptation. The morphological knowledge of the tongue and laryngeal entrance of ducks, particularly *A. crecca*, is limited, with only a few recent articles providing insights into the tongue and the laryngeal mound in some duck species (Abumandour et al., 2019; Skieresz-Szewczyk & Jackowiak, 2016; Skieresz-Szewczyk et al., 2014; Skieresz-Szewczyk et al., 2014); however, the oropharyngeal cavity roof is completely described in *A. crecca* by (Alruhaimi et al., 2024).

The tongue plays a crucial role in collecting, filtration, processing, and movement of the food particles towards the esophagus, as described in food intake feeding behavior in avian species. These different lingual functions reflect the lingual appearance and ultrastructural features (Erdogan & Iwasaki, 2014). There is a species-specific characteristic of the lingual appearance that has adapted to specific feeding habits and the types of available food particles (Erdogan & Iwasaki, 2014). Our description of an elongated, wide tongue with a free apex and a strong lingual frenulum fixation to the oropharyngeal cavity floor is similar to those described in all waterbirds, including the domestic duck and goose (Iwasaki et al., 1997; Jackowiak et al., 2011; Skieresz-Szewczyk & Jackowiak, 2016; Skieresz-Szewczyk et al., 2014), and the omnivorous Garganey (Abumandour et al., 2019). Avian species have elongated, narrow tongues for carnivorous behaviors (Abumandour & El-Bakary, 2017b; Emura et al., 2008a), herbivorous behaviors (Abumandour, 2018; Abumandour & El-Bakary, 2019b), and migratory behaviors of the coots (Abumandour & El-Bakary, 2017a), while triangular tongues are used for herbivorous behaviors in *Galliformes*, *Passerines*, and *Columbiformes* (Abumandour & El-Bakary, 2019a; Abumandour, El-Bakary, et al., 2021; Abumandour & Kandyel, 2020; Dehkordi et al., 2010; El-Mansi et al., 2021). Some birds exhibit different tongue shapes, such as the oval tongue in Middendorf's bean goose (Iwasaki et al., 1997), the brush-like tongue in the hummingbirds (Rico-Guevara & Rubega, 2011), the mushroom tongue in the cormorants (Jackowiak et al., 2006), a toothpick tongue in the Japanese pygmy woodpecker (Emura et al., 2009), and the needle-shaped tongue in the Little Egret and heron (Emura, 2009). The longer tongue than the lower jaw is seen in the woodpecker (Emura et al., 2009), while there are two cases of short according to its adaptations; the short primitive nonfunctional tongue is seen in hoopoes and ratites (Abumandour & Gewaily, 2019a; Crole & Soley, 2010b; Jackowiak & Ludwig, 2008b; Santos et al., 2011), and the short functionally movable tongue is seen in Egyptian nightjars (El-Mansi et al., 2020) and the Eurasian collared dove (El-Mansi et al., 2021).

The lingual apex is closely linked to avian dietary habits and is responsible for various functions in various feeding techniques, including food collection and manipulation (Abumandour, Farrag, et al., 2021; Bassuoni et al., 2022; El-Mansi et al., 2021; Erdogan & Iwasaki, 2014; Gewaily & Abumandour, 2020). Our description of the spatula-like nail of the lingual apex of *Anas crecca* is similar to those described in most water birds, including ducks and geese (Abumandour et al., 2019; Jackowiak et al., 2021; Jackowiak et al., 2011; Marzban Abbasabadi & Sayrafi, 2018; Skieresz-Szewczyk & Jackowiak, 2016), but is absent in some waterbird species like the coot and moorhen (Abumandour & El-Bakary, 2017a; Bassuoni et al., 2022). Previous data revealed some anatomical adaptations of the apex, including numerous rostrally directed acicular processes on the rostral and lateral borders of the rounded apex of moorhens, coots, Japanese pygmy woodpeckers, and magpies (Abumandour & El-Bakary, 2017; Bassuoni et al., 2022; Emura et al., 2009; Erdogan et al., 2012), while, the ratites have a smooth apex (Jackowiak & Ludwig, 2008a; Santos et al., 2011), but Egyptian nightjars have a blunt apex (El-Mansi et al., 2020), whilst the Eurasian Collared Dove tongue has a spear-like apex (El-Mansi et al., 2021). However, the nutcracker's apex has two dagger-like processes for catching, raising, and putting seeds on the median lingual groove (Jackowiak et al., 2010). The bifid apex is found in carnivorous birds like the little tern, owl, peregrine falcon, and kestrel (Emura & Chen, 2008; EMURA et al., 2008b; Iwasaki, 1992) and some herbivorous birds like the red jungle fowl and magpie (Erdogan et al., 2012; Kadhim et al., 2011), while the pointed apex is found in the chicken and the zebra finch (Dehkordi et al., 2010; Iwasaki & Kobayashi, 1986).

Our study revealed that the lingual feeding filtering apparatus is classified as lateral and dorsal papillary apparatus, in which the lateral apparatus has numerous mechanically conical papillae, including long and hair-like filiform papillae, which filter food particles from water streams during ejection, while the dorsal apparatus has ridged-like and rod-like papillae, along with small papillae of the papillary crest and spinated border of the root, which move food particles with water to the lateral sides of the prominence. Our study revealed that the feeding filtering apparatus has eight papillary types: ridge-like, small pointed, rod-like, small conical, large quadrilateral, large triangular, small triangular, and hair-like filiform papillae. Meanwhile, the domestic duck's feeding filtering apparatus consists of three papillary types: small conical and filiform papillae on the rostral part of the body, large conical papillae on the caudal part of the body, and conical papillae on the lingual prominence (Skieresz-Szewczyk & Jackowiak, 2016), while Abumandour et al. (2019) revealed three papillary types: hair-like papillae on the lateral tip surface, rostral, and middle parts of the body; small conical papillae on the lateral surface of the rostral and middle parts and prominence; and large conical papillae on the lateral surface of the caudal part of the body and prominence in the Garganey. Previous studies have described numerous hair-like filiform papillae on the lateral border of the lingual prominence in the Garganey, domestic duck, and geese tongues (Abumandour et al., 2019; Iwasaki et al., 1997; Jackowiak et al., 2011; Skieresz-Szewczyk & Jackowiak, 2014).

Our description of the papillary distribution included that the two lateral apical regions (except the nail) has numerous ridge-like and small pointed filiform papillae on their lateral surfaces, and the rostral part of the pyramidal region (before the lingual comb) has numerous rod-like filiform, small conical, and ventral rod-like filiform papillae on its lateral surfaces, while the large part of the pyramidal region has a lingual comb, randomly spines, round and elongated tubercles, the numerous small filiform papillae on its dorsal surface, and its lateral surface carried numerous large quadrilateral conical papillae rostrally and large triangular conical papillae with numerous hair-like filiform papillae caudally just at the level of the head and caudal part of the lingual comb. Furthermore, the lingual prominence's dorsal surface has a lateral serrated border on its rostral part of the lateral portion, while its caudal part carries a wedge-shape structure, and the lateral surface of the prominence carries large triangular conical, hair-like, and ventral rod-like filiform papillae at its rostral part, while its caudal part has numerous small pointed filiform papillae. Also, the lingual root has numerous spinated borders from all sides: the papillary crest rostrally, the lateral serrated border laterally, and caudally by the dorsal spinated border, which is divided into two halves (right and left).

The *Anseriformes* have slight variations in the appearance of their lingual groove on their dorsal surface. Our results show that the rostral ¾ part of the lingual prominence has a shallow median groove, but the caudal ¼ part is devoid of this groove, similar to domestic ducks (Skieresz-Szewczyk & Jackowiak, 2016). The lingual prominence in Garganey and domestic goose has a median groove along its dorsal surface (Abumandour et al., 2019; Jackowiak et al., 2011), while in domestic goose, it only appears on the median portion (Skieresz-Szewczyk et al., 2021). Our study reveals that the lingual groove begins and ends as a shallow groove, but it appears as a triangular groove on the apex and rostral part of the body with a central deep groove, and it appears as a single deep groove at the lingual comb. Meanwhile, the groove extends along the dorsal surface of the apex and body, where it is deep in the rostral ⅔ and shallow in the caudal ⅓ of the tongue on the lingual prominence in Garganey and coot (Abumandour et al., 2019; Abumandour & El-Bakary, 2017a). However, it is a shallow groove on the body and the lingual prominence in domestic ducks (Skieresz-Szewczyk & Jackowiak, 2016), whereas it is only on the dorsal surface of the body in the domestic goose (Jackowiak et al., 2011), only on the rostral part of the body without the apex and prominence in the Middendorff’s bean goose (Iwasaki et al., 1997), only on the apex and body in the Eurasian Collared Dove (El-Mansi et al., 2021), and only on the apex in the Egyptian nightjar (El-Mansi et al., 2020). The groove is absent in certain birds with varying feeding habits, such as the penguin, Rhea americana, and Egyptian laughing dove (Abumandour & El-Bakary, 2019b; Kobayashi et al., 1998; Santos et al., 2011).

The rectangular lingual prominence, with its papillary crest and its role as typical lingual structure in the filter feeding technique, has been described in our study as well as on the tongue of *Anseriformes*, including domestic and wild duck (Abumandour et al., 2019; Skieresz-Szewczyk & Jackowiak, 2016; Skieresz-Szewczyk et al., 2014) and domestic geese (Jackowiak et al., 2011; King & McLelland, 1984). The lingual prominence functions as a "fat cushion" that absorbs forces from eating and transporting food by placing it against the palate (Jackowiak et al., 2011; Kooloos et al., 1989) and pressing on the lingual glands to secrete mucus (Jackowiak et al., 2011; Kooloos et al., 1989). Our study confirms the role of lingual prominence and root in the feeding filter apparatus by observing the arrangement of various papillary types, in which the rostral part of the lateral portion of the prominence has a serrated border of 10–12 small triangular pointed processes, while its caudal part has a wedge-shaped structure; additionally, its lateral surface carries large triangular pointed processes. Moreover, the short lingual root is completely bordered by numerous spinated borders: the papillary crest rostrally, the lateral serrated border laterally, and the dorsal spinated border caudally.

The papillary crest, a fundamental part of lingual structures in most birds of the different nutritional mechanisms (Abumandour & Kandyel, 2020; Abumandour, Farrag, et al., 2021; El-Mansi et al., 2020; El-Mansi et al., 2021; Iwasaki et al., 1997; Marzban Abbasabadi & Sayrafi, 2018; Skieresz-Szewczyk & Jackowiak, 2016), is absent in some birds like the penguin, Japanese pygmy woodpecker, and Rhea Americana (Emura et al., 2009; Kobayashi et al., 1998; Santos et al., 2011). We agree with the former data that the papillary crest plays a crucial role in preventing food particles from rostral escape and directing them towards the esophagus (Abumandour & El-Bakary, 2019a; Abumandour & El-Bakary, 2017a; Abumandour & El-Bakary, 2017b; El-Mansi et al., 2021; Jackowiak et al., 2011). The study reveals minor variations in the crest among avian species, including shape, number of papillary rows, and direction. Our study describes two transverse papillary rows: the dorsal row of 16–18 large triangular papillae and the ventral row of 14–16 small papillae. Papillary crest formation from two transverse papillary rows is common in *Anseriformes* like domestic ducks (Skieresz-Szewczyk & Jackowiak, 2016) and some avian species like kestrels, owls, and sparrows (Abumandour, 2018; Abumandour & El-Bakary, 2017b), while one transverse papillary row is found in coots, quails, and Eurasian collared doves (Abumandour & El-Bakary, 2017a; Abumandour, Farrag, et al., 2021; El-Mansi et al., 2021). The V-crest is the most common crest shape in birds, including sparrows, Hobby, and Northern Pintail (Abumandour, 2018; Abumandour, 2014; El Bakary, 2015), while, the W-crest is observed in the hoopoe (El-Bakary, 2011), but the U-crest in the cattle egret and Egyptian nightjar (Al-Ahmady Al-Zahaby, 2016; El-Mansi et al., 2020). Our findings revealed the characteristic short root in the *Anatoidea*, in which it is divided into two halves (right and left) by a narrow median passway, leaving a small smooth semilunar area, as in Garganey and domestic ducks (Abumandour et al., 2019; Skieresz-Szewczyk & Jackowiak, 2016). The lingual root of the coot has four portions: round, triangular, semilunar, and depressed (Abumandour & El-Bakary, 2017a), while the root is classified into two portions: the rostral V-portion and caudal wide portion in the sparrow (Abumandour, 2018). Meanwhile, the root of the kestrel was formed from one portion of a U-shape (Abumandour & El-Bakary, 2017b) and a V-shape in the Hume's tawny owl.

The laryngeal entrance is neglected in previously published articles on all *Anatoidea*, except that described in garganey (Abumandour et al., 2019) and also in other avian species (Abumandour & El-Bakary, 2019a; Abumandour, 2014; El-Mansi et al., 2020; El-Mansi et al., 2021). Our study gave a specific classification of the laryngeal region into the papillary (pre-glottic) triangular and the non-papillary (glottic) elevated areas, similar to that described in Garganey (Abumandour et al., 2019). Our study provides a fantastic subdivision of the papillary area into the lateral papillary portion with a small number of sphenopalatine salivary glands and the median smooth portion with three slightly oblique papillary rows that have not previously been described in any avian species. Meanwhile, the papillary area of the Garganey has numerous randomly distributed caudally and caudolaterally oriented small conical papillae and a median non-papillary longitudinal ridge (Abumandour et al., 2019).

Our findings show that the elevated laryngeal mound with its median glottic opening and two non-papillary glandular plates is bordered caudally by the pharyngeal papillae, similar to those previously described in the pigeon, moorhen, Egyptian nightjar, and Eurasian Collared Dove (Abumandour, El-Bakary, et al., 2021; Bassuoni et al., 2022; El-Mansi et al., 2020; El-Mansi et al., 2021). Minor variations exist in the mound and its glottic opening appearance among various avian species. Our findings reveal the ovoid mound being similar to the mound of the moorhen (Bassuoni et al., 2022) and hobby (Abumandour, 2014), the circular, conspicuous, and fleshy mound found in the Eurasian collared dove (El-Mansi et al., 2021), and the rectangular mound in quail (Abumandour, Farrag, et al., 2021), while the triangular mound is the most famous among avian species (Abumandour, 2018; Abumandour, 2014; Abumandour & El-Bakary, 2017a; Abumandour & El-Bakary, 2017b; El-Mansi et al., 2020; Erdogan & Alan, 2012). Moreover, our findings reveal an ovoid, wide glottic opening with a papillary border of 10–12 conical papillae, extending as a laryngeal fissure with 2-4 papillae on each side, bordered by a longitudinal pharyngeal papillary row of large conical papillae. The ovoid opening is also described in the hoopoe and Eurasian collared dove (Abumandour & Gewaily, 2019b; El-Mansi et al., 2021), the elongated opening found in the Garganey (Abumandour et al., 2019), the elliptical glottic opening observed in the moorhen (Bassuoni et al., 2022), and the elongated triangular shape seen in the coot (Abumandour & El-Bakary, 2017). Our descried papillary border surrounding the glottic opening has been reported in some birds, including the Garganey, quail, Egyptian laughing dove, and sparrow (Abumandour, 2018; Abumandour et al., 2019; Abumandour & El-Bakary, 2019b; Abumandour, Farrag, et al., 2021; El-Mansi et al., 2021), while the non-papillary border is found in some avian species, including the moorhen, the Egyptian nightjar, and hobby (Abumandour, 2014; Bassuoni et al., 2022; El-Mansi et al., 2020), but there are papillae surrounding the caudal portion of the glottic opening only, as in the Eurasian coot (Abumandour & El-Bakary, 2017).

Our study provides that the fantastic diamond-shape pharyngeal papillae are arranged in 7-8 transverse papillary rows and one longitudinal papillary row of the caudally directed mechanical conical papillae. The diamond-shaped pharyngeal papillae are also described in the Garganey (Abumandour et al., 2019), while the heart-shaped pharyngeal papillae are in the coot (Abumandour & El-Bakary, 2017a). Meanwhile, the pharyngeal papillae are observed as one transverse papillary row in some birds (Abumandour & Gewaily, 2019b; Mahdy, 2020), but the two transverse papillary rows are found in the Egyptian nightjar (El-Mansi et al., 2020) and the magpie and raven (Erdogan & Alan, 2012), while the three semilunar papillary rows are found in the common moorhen (Bassuoni et al., 2022).

Meanwhile, the pharyngeal papillae disappeared completely in ratites (Crole & Soley, 2010a). Our work confirmed what has previously been reported about the important role of these pharyngeal papillae in the caudal direction of the caught and filtrated nutrient materials toward the esophagus (Abumandour, 2018; Abumandour & El-Bakary, 2019b; Abumandour & El-Bakary, 2017a).

5. Conclusion

Our study is the first morphological effort to characterize the tongue and laryngeal mound adaptations with their species-specific feeding behaviors, to identify the feeding filtering technique in *A. crecca*. The feeding apparatus is formed by the lateral and dorsal papillary systems. The lateral papillary system had conical papillae with numerous long filiform and hair-like filiform papillae to constitute the food filtration apparatus, while the dorsal papillary system had ridged-like and rod-like papillae in addition to the small papillae of the papillary crest and spinated border of the root to help in moving the food particles with water to the lateral sides of the prominence. The papillary laryngeal area had two lateral papillary portions of the caudolaterally directed papillae and the median smooth portion. Consequently, tongue and laryngeal mound ultrastructure exhibits anatomical adaptations for efficiently filtering feeding mechanisms.

Declarations

Ethics approval and consent to participate

This study was carried out according to the Institutional Animal Care and Use Committee (IACUC) protocols of Laboratory Animals, Faculty of Veterinary Medicine, Alexandria University (Approval No.: 11/3/2023/231). All methods were performed in accordance with relevant guidelines and regulations by the Basel Declaration and the International Council for Laboratory Animal Science (ICLAS). The anatomical nomenclature was applied according to ***Nomina Anatomica Avium*** (1993)

Consent for publication: Not applicable.

Availability of data and materials:

The datasets used and/or analyzed during the current study are available from the corresponding author on reasonable request. The manuscript contains all data supporting the reported results.

Competing interests:

None of the authors has any financial or personal relationships that could inappropriately influence or bias the content of the paper.

Funding:

Princess Nourah bint Abdulrahman University Researchers Supporting Project Number (PNURSP2024R381), Princess Nourah bint Abdulrahman University, Riyadh, Saudi Arabia.

Authors' contributions

RSA, Reem S. Alruhaimi. MA, Mohamed Abumandour. **MK**, Mohammed Kassab. **AAE**, Ahmed A. Elnegiry. **FF**, Foad Farrag. **DM**, Diaa Massoud. **AMM**, Ayman M. Mahmoud. **BHA,** Bandar H. AL-Osaimi. **HH**, Hazem Hamoda. **MA, HH, AAE, and FF** wrote the manuscript and interpreted the results, **MA, FF, DM, BH, and AMM** collected the samples, performed the scanning electron examinations, **MA, HH, and MK** prepared the figures, and **MA, RSA, HH, and AAE** assisted in interpreting the results. **MA, FF, DM, BHA, RSA, and AAE** prepared the revised version and statistical analysis. All authors reviewed the manuscript.

Acknowledgments

Princess Nourah bint Abdulrahman University Researchers Supporting Project Number (PNURSP2024R381), Princess Nourah bint Abdulrahman University, Riyadh, Saudi Arabia.

6. References:

Abumandour, M., & El-Bakary, N. J. A., histologia, embryologia. (2017). Morphological characteristics of the oropharyngeal cavity (tongue, palate and laryngeal entrance) in the Eurasian coot (Fulica atra, Linnaeus, 1758). *46*(4), 347-358.

Abumandour, M. M. (2018). Surface ultrastructural (SEM) characteristics of oropharyngeal cavity of house sparrow (Passer domesticus). *Anat Sci Int, 93*(3), 384-393.

Abumandour, M. M., Bassuoni, N. F., & Hanafy, B. G. (2019). Surface ultrastructural descriptions of the oropharyngeal cavity of Anas querquedula. *Microscopy research and technique, 82*(8), 1359-1371.

Abumandour, M. M., & El-Bakary, N. E. (2019a). Anatomical investigations of the tongue and laryngeal entrance of the Egyptian laughing dove Spilopelia senegalensis aegyptiaca in Egypt. *Anat Sci Int, 94*(1), 67-74.

Abumandour, M. M., & El-Bakary, N. E. (2019b). Anatomical investigations of the tongue and laryngeal entrance of the Egyptian laughing dove Spilopelia senegalensis aegyptiaca in Egypt. *Anat Sci Int, 94*(1), 76-74.

Abumandour, M. M., El-Bakary, N. E., Elbealy, E. R., El-Kott, A., Morsy, K., Haddad, S. S., Madkour, N., & Kandyel, R. M. (2021). Ultrastructural and histological descriptions of the oropharyngeal cavity of the rock pigeon Columba livia dakhlae with special refer to its adaptive dietary adaptations. *Microscopy research and technique, 84*(12), 3116-3127. doi:https://doi.org/10.1002/jemt.23870

Abumandour, M. M., & Gewaily, M. S. (2019a). Gross morphological and ultrastructural characterization of the oropharyngeal cavity of the Eurasian hoopoe captured from Egypt. *Anat Sci Int, 94* (2), :172-179. doi:0.1007/s12565-018-0463-9

Abumandour, M. M., & Kandyel, R. M. (2020). Age-related ultrastructural features of the tongue of the rock pigeon Columba livia dakhlae in different three age stages (young, mature, and adult) captured from Egypt. *Microscopy research and technique, 83*, 118–132. doi:https://doi.org/10.1002/jemt.23394

Abumandour, M. M. A. (2014). Gross Anatomical Studies of the Oropharyngeal Cavity in Eurasian Hobby (Falconinae: Falco Subbuteo, Linnaeus 1758). *J Life Sci Res, 1*(4), 80-92.

Abumandour, M. M. A., & El-Bakary, N. E. R. (2017a). Morphological Characteristics of the Oropharyngeal Cavity (Tongue, Palate and Laryngeal Entrance) in the Eurasian Coot (Fulica atra, Linnaeus, 1758). *Anat Histol Embryol, 46*(4), 347-358. doi:10.1111/ahe.12276

Abumandour, M. M. A., & El-Bakary, N. E. R. (2017b). Morphological features of the tongue and laryngeal entrance in two predatory birds with similar feeding preferences: common kestrel (Falco tinnunculus) and Hume's tawny owl (Strix butleri). *Anat Sci Int, 92*(3), 352–363. doi:10.1007/s12565-016-0339-9

Abumandour, M. M. A., Eldefrawy, F., Morsy, K., El-Bakary, N., & Hanafy, B. G. (2023). Scanning electron microscopic characterizations of the tongue of the Nubian goat (Capra aegagrus hircus): A specialized focus on its papillary system adaptation to Egyptian environmental conditions. *Anatomia, histologia, embryologia*. doi:https://doi.org/10.1111/ahe.12915

Abumandour, M. M. A., Farrag, F. A., El-Mansi, A., Lashen, S. E., Shukry, M., Kassab, M. A., & Hamoda, H. S. (2021). Posthatching developmental studies on the tongue and laryngeal entrance of the common quail (Coturnix coturnix, Linnaeus, 1758) in different five age-stages. *Microscopy research and technique, 84*(8), 1649–1672. doi:10.1002/jemt.23885

Abumandour, M. M. A., & Gewaily, M. S. (2019b). Gross morphological and ultrastructural characterization of the oropharyngeal cavity of the Eurasian hoopoe captured from Egypt. *Anat Sci Int, 94*(2), 172-179. doi:10.1007/s12565-018-0463-9

Abumandour, M. M. A., Haddad, H., Farrag, F., Kandyel, R. M., Roshdy, K., Massoud, D., & Khalil, E. K. (2024). Biological aspects of the lingual papillae of the Arab Zebu cattle: a new perspicuity of its chad ecological adaptations. *BMC Zoology, 9*(1), 21. doi:https://doi.org/10.1186/s40850-024-00208-w

Abumandour, M. M. A., & Hanafy, B. G. (2024). Gross and scanning electron microscopic features of the oral cavity (palate, tongue, and sublingual floor) of the Egyptian long-eared hedgehog (Hemiechinus auratus aegyptius). *BMC veterinary research*.

Al-Ahmady Al-Zahaby, S. (2016). Light and scanning electron microscopic features of the tongue in cattle egret. *Microsc Res Tech, 79*(7), 595-603.

Alruhaimi, R. S., Abumandour, M. M. A., Kassab, M., Elnegiry, A. A., Farrag, F., Massoud, D., Mahmoud, A. M., & Hamoda, H. (2024). Structural adaptations of the beak and oropharyngeal cavity roof in migratory Anas crecca: Distinctive scanning electron microscopic pattern of its filter feeding apparatus. *Zoologischer Anzeiger, 311*, 1-15. doi:https://doi.org/10.1016/j.jcz.2024.05.004

Bassuoni, N. F., Abumandour, M. M. A., Morsy, K., & Hanafy, B. G. (2022). Ultrastructural adaptation of the oropharyngeal cavity of the Eurasian common moorhen (Gallinula chloropus chloropus): Specific adaptive dietary implications. *Microscopy research and technique, 85*(5), 1915–1925. doi:https://doi.org/10.1002/jemt.24053

Baumel, J. J., King, S. A., Breazile, J. E., Evans, H. E., & Berge, J. C. V. (1993). *Handbook of avian anatomy: Nomina Anatomica Avium. 2nd ed.* . Cambridge: Nuttall Ornithological Club. 779p.

Baussart, S., & Bels, V. (2011). Tropical hornbills (Aceros cassidix, Aceros undulatus, and Buceros hydrocorax) use ballistic transport to feed with their large beaks. *Journal of Experimental Zoology Part A: Ecological Genetics, 315*(2), 72-83.

Bels, V., & Baussart, S. J. F. i. d. v. f. s. t. b. W. C. P., UK p. (2006). Feeding behaviour and mechanisms in domestic birds. 33-50.

BirdLife International. (2020). *Anas crecca. The IUCN Red List of Threatened Species 2020: e.T22680321A181692388. https://dx.doi.org/10.2305/IUCN.UK.2020-3.RLTS.T22680321A181692388.en.* Retrieved from

Crole, M. R., & Soley, J. T. (2010a). Gross Morphology of the Intra-Oral rhamphotheca, Oropharynx and Proximal Oesophagus of the Emu (Dromaius novaehollandiae). *Anat Histol Embryol, 39* 207–218. doi:10.1111/j.1439-0264.2010.00998.x

Crole, M. R., & Soley, J. T. (2010b). Surface morphology of the emu (Dromaius novaehollandiae) tongue. *Anat Histol Embryol, 39*, 355-365.

Dehkordi, R. A. F., Parchami, A., & Bahadoran, S. (2010). Light and scanning electron microscopic study of the tongue in the zebra finch Cardueis carduelis (Aves: Passeriformes: Fringillidae). *Slov Vet Res, 47*, 139-144.

Dimech, M., Stamatopoulos, C., El-Haweet, A. E., Lefkaditou, E., Mahmoud, H. H., Kallianiotis, A., & Karlou-Riga, C. (2012). Sampling protocol for the pilot collection of catch, effort and biological data in Egypt. Food and Agriculture Organization of the United Nations. *EastMed Technical Documents*. doi:https://www.fao.org/publi catio ns/card/en/c/2f11c e49-f36a-5f43-8f66-d77b2 388d8 93/

El-Bakary, N. E. R. (2011). Surface morphology of the tongue of the hoopoe (Upupa epops). *J Am Sci, 7*, 394–399.

El-Mansi, A., Al-Kahtani, M., Abumandour, M., Ezzat, A., & El-Badry, D. (2020). Gross anatomical and ultrastructural characterization of the oropharyngeal cavity of the Egyptian nightjar Caprimulgus aegyptius: Functional dietary implications. *Ornithological Science, 19*(2), 145-158.

El-Mansi, A. A., El-Bealy, E. A., Al-Kahtani, M. A., Al-Zailaie, K. A., Rady, A. M., Abumandour, M. A., & El-Badry, D. A. (2021). Biological Aspects of the Tongue and Oropharyngeal Cavity of the Eurasian Collared Dove (Streptopelia decaocto, Columbiformes, Columbidae): Anatomical, Histochemical, and Ultrastructure Study. *Microscopy and Microanalysis, 27*(5), 1234-1250. doi:10.1017/S1431927621012101

El Bakary, E. S. N. R. (2015). Morphology of the oropharyngeal cavity of Northern pintail (Anas acuta). *Global Veterinaria, 14*, 459-464.

Elghoul, M., Morsy, K., & Abumandour, M. M. A. (2022). Ultrastructural characterizations of the pecten oculi of the common ostrich (Struthio camelus): New insight to scanning electron microscope–energy dispersive X-ray analysis. *Microsc Res Tech, 85*(5), 1654-1662.

Emura, S. (2009). SEM studies on the lingual dorsal surfaces in three species of herons (in Japanese). *Med Biol, 153*, 423−430.

Emura, S., & Chen, H. J. A., histologia, embryologia. (2008). Scanning electron microscopic study of the tongue in the owl (Strix uralensis). *37*(6), 475-478.

Emura, S., Okumura, T., & Chen, H. (2008a). Scanning electron microscopic study of the tongue in the Peregrine falcon and Common kestrel. *Okajimas Folia Anat Jpn, 85*, 11-15.

Emura, S., Okumura, T., & Chen, H. (2009). Scanning electron microscopic study of the tongue in the Japanese pygmy woodpecker (Dendrocopos kizuki). *Okajimas Folia Anat Jpn, 86*, 31-35.

EMURA, S., OKUMURA, T., & CHEN, H. J. O. f. a. J. (2008b). Scanning electron microscopic study of the tongue in the peregrine falcon and common kestrel. *85*(1), 11-15.

Erdogan, S., & Alan, A. (2012). Gross anatomical and scanning electron microscopic studies of the oropharyngeal cavity in the European magpie (Pica pica) and the common raven (Corvus corax). *Microsc Res Tech, 75*, 379–387.

Erdogan, S., Alan, A. J. M. r., & technique. (2012). Gross anatomical and scanning electron microscopic studies of the oropharyngeal cavity in the European magpie (Pica pica) and the common raven (Corvus corax). *75*(3), 379-387.

Erdogan, S., & Iwasaki, S. (2014). Function-related morphological characteristics and specialized structures of the avian tongue. *Annals of Anatomy, 196*, 75-87. doi:10.1016/j.aanat.2013.09.005

Gewaily, M. S., & Abumandour, M. M. (2020). Gross morphological, histological and scanning electron specifications of the oropharyngeal cavity of the hooded crow (Corvus cornix pallescens). *Anatomia, histologia, embryologia, 50*(1), 72-83.

Iwasaki, S.-i., & Kobayashi, K. J. A. a. n. (1986). on the Lingual Dorsal Epithelium of Chickens. *61*(2), 83-96.

Iwasaki, S., Tomoichiro, A., & Akira, C. (1997). Ultrastructural study of the keratinization of the dorsal epithelium of the tongue of Middendorff's bean goose, Anser fabalis middendorffii (Anseres, Anatidae). *Anat Rec, 247*, 149-163.

Iwasaki, S. I. J. J. o. M. (1992). Fine structure of the dorsal lingual epithelium of the little tern, Sterna albifrons Pallas (Aves, Lari). *212*(1), 13-26.

Jackowiak, H., Andrzejewski, W., & Godynicki, S. (2006). Light and scanning electron microscopic study of the tongue in the cormorant Phalacrocorax carbo (Phalacrocoracidae, Aves). *Zool Sci, 23*, 161-167.

Jackowiak, H., & Ludwig, M. (2008a). Light and scanning electron microscopic study of the structure of the ostrich (Strutio camelus) tongue. *Zoological Science, 25*(2), 188-194.

Jackowiak, H., & Ludwig, M. (2008b). Light and scanning electron microscopic study of the structure of the ostrich (Strutio camelus) tongue. *Zool Sci, 25*, 188-194.

Jackowiak, H., Skieresz-Szewczyk, K., Godynicki, S., Iwasaki, S., & Meyer, W. (2021). Functional morphology of the tongue in the domestic goose (Anser anser f. domestica). . 2011 Sep;(9):1574-84. doi: 10.1002/ar.21447. Epub 2011 Aug 9. PMID: 21830308. *Anat Rec (Hoboken), 294*(9). doi:10.1002/ar.21447

Jackowiak, H., Skieresz-Szewczyk, K., Kwiecin´ ski, Z., Trzcielin´ skaLorych, J., & Godynicki, S. (2010). Functional morphology of the tongue in the nutcracker (Nucifraga caryocatactes). *Zool Sci, 27*, 589-594.

Jackowiak, H., Skieresz-Szewczyk, K., Godynicki, S., Iwasaki, S. i., & Meyer, W. (2011). Functional morphology of the tongue in the domestic goose (Anser anser f. domestica). *Anat Rec, 294*(9), 1574-1584.

Kadhim, K. K., Zuki, A., Babjee, S., Noordin, M., & Zamri-Saad, M. J. A. J. o. B. (2011). Morphological and histochemical observations of the red jungle fowl tongue Gallus gallus. *10*(48), 9969-9977.

Kandyel, R. M., Choudhary, O. P., El-Nagar, S. H., Miles, D. B., & Abumandour, M. M. A. (2023). Tongue of the Egyptian Endemic Bridled Skink (Heremites vittatus; Olivier, 1804): Gross, Electron Microscopy, Histochemistry, and Immunohistochemical Analysis. *Animals, 13*(21), 3336. doi:https://doi.org/10.3390/ani13213336

Kandyel, R. M., El Basyouny, H. A., Albogami, B., Madkour, N. F., & Abumandour, M. M. A. (2024). Comparative ultrastructural study of the oropharyngeal cavity roof in Tarentola annularis and Heremites vittatus: To special reference to palate adaptation with feeding habits. *Zoologischer Anzeiger, 308*, 57-65. doi:https://doi.org/10.1016/j.jcz.2023.11.004

Kandyel, R. M., El Basyouny, H. A., El-Nagar, S., Madkour, N. F., Massoud, D., Almadiy, A. A., Albogami, B., Alasmari, S., & Abumandour, M. M. A. (2024). Lingual adaptations of the Tarentola annularis with new insights into its papillary system adaptations: Ultrastructure, histochemistry, and immunohistochemical observations. *Tissue and Cell, 88*, 102366. doi:https://doi.org/10.1016/j.tice.2024.102366

Kandyle, R., El Basyouny, H. A., Morsy, K., Abourashed, N. M., Madkour, N., & Abumandour, M. M. A. (2022). Gross, ultrastructural, and histological characterizations of pecten oculi of the glossy ibis (Plegadis falcinellus): New insights into its scanning electron microscope–energy dispersive X-ray analysis. *Microscopy research and technique, 85*(12), 3908-3920. doi:0.1002/jemt.24228

King, A. S., & McLelland, J. (1984). *Birds, their structure and function*: Bailliere Tindall, 1 St. Annes Road.

Kobayashi, K., Kumakura, M., Yoshimura, K., Inatomi, M., & Asami, T. (1998). Fine structure of the tongue and lingual papillae of the Penguin. *Arch Histol Cytol, 61*, 37-46.

Kooloos, J., Kraaijeveld, A., Langenbach, G., & Zweers, G. J. Z. (1989). Comparative mechanics of filter feeding in Anas platyrhynchos, Anas clypeata and Aythya fuligula (Aves, Anseriformes). *108*(5), 269-290.

Madge, S., & Burn, H. (1988). *Wildfowl: an identification guide to the ducks, geese and swans of the world*: A&C Black.

Mahdy, M. A. (2020). Comparative morphological study of the oropharyngeal floor of squabs and adult domestic pigeons (Columba livia domestica). *Microscopy research and technique*.

Marzban Abbasabadi, B., & Sayrafi, R. (2018). Histomorphological features of the tongue of the Eurasian teal (Anas crecca). *Anatomia, histologia, embryologia, 47*(2), 119-123.

Massoud, D., Fouda, M., Shaldoum, F., Alrashdi, B. M., AbdRabou, M. A., Soliman, S. A., Abd-Elhafeez, H. H., Hassan, M., & Abumandour, M. M. A. (2023). Characterization of the Small Intestine in the Southern White-breasted Hedgehog (Erinaceus concolor) Using Histological, Histochemical, Immunohistochemical, and Scanning Electron Microscopic Techniques. *Microscopy and Microanalysis, 29*(6), 2218–2225. doi:https://doi.org/10.1093/micmic/ozad128

Rico-Guevara, A., & Rubega, M. A. (2011). The hummingbird tongue is a fluid trap, not a capillary tube. *Proc Natl Acad Sci USA, 108* (23), 9356–9360.

Roshdy, K., Morsy, K., & Abumandour, M. M. (2021). Microscopic focus on ependymal cells of the spinal cord of the one-humped camel (Camelus dromedarius): Histological, immunohistochemical, and transmission microscopic study. *Microscopy research and technique, 85*(4), 1238-1247. doi:https://doi.org/10.1002/jemt.23990

Santos, T. C., Fukuda, K. Y., Guimara˜es, J. P., Oliveira, M. F., Miglino, M. A., & Watanabe, L. (2011). Light and scanning electron microcopy study of the tongue in Rhea americana. *Zool Sci, 28*, 41-46.

Schneider, C. A., Rasband, W. S., & Eliceiri, K. W. (2012). NIH Image to ImageJ: 25 years of image analysis. *Nature methods, 9*(7), 671-675.

Schwenk, K., & Rubega, M. (2005). Diversity of vertebrate feeding systems. *Physiological and ecological adaptations to feeding in vertebrates*, 1-41.

Skieresz-Szewczyk, K., & Jackowiak, H. (2014). Scanning electron microscopy investigation of the filter-feeding apparatus in the domestic goose (Anser anser f. domestica) and the domestic duck (Anas platyrhynchos f. domestica). *Microscopy: advances in scientific research and education (A. Méndez-Vilas, Ed.), 1*, 2014.

Skieresz-Szewczyk, K., & Jackowiak, H. (2016). Morphofunctional study of the tongue in the domestic duck (Anas platyrhynchos f. domestica, Anatidae): LM and SEM study. *Zoomorphology, 135*(2), 255-268.

Skieresz-Szewczyk, K., Jackowiak, H., & Ratajczak, M. (2014). LM and TEM study of the orthokeratinized and parakeratinized epithelium of the tongue in the domestic duck (Anas platyrhynchos f. domestica). *Micron, 67*, 117-124.

Skieresz-Szewczyk, K., Jackowiak, H., & Ratajczak, M. J. S. R. (2021). Unique pattern of histogenesis of the parakeratinized epithelium on lingual prominence in the domestic goose embryos (Anser anser f. domestica). *Scientific Reports, 11*(1), 1-16. doi:https://doi.org/10.1038/s41598-021-02020-9

Skieresz-Szewczyk, K., Jackowiak, H., & Kontecka, H. (2014). Morphogenesis of the tongue mucosa in the domestic duck (Anas platyrhynchos f. domestica) during the late embryonic stages. *Microscopy research and technique, 77*(9), 667-674.

Tadjalli, M., Mansouri, S. H., & Poostpasand, A. (2008). Gross anatomy of the oropharyngeal cavity in the ostrich (Struthio camelus). *Iranian J Vet Res, 9*(4 (25)), 316-323.

Tawfiek, M. G., & Mahmoud, H. H. (2020). Gross Morphology and Scanning Electron Microscopic Structure of the Oropharyngeal Cavity of the Domestic Geese (Anser anser domesticus). *Journal of Veterinary Medical Research, 27*(2), 190-202. doi:https://doi.org/10.21608/JVMR.2021.61981.1034

Tomlinson, B. C. A. (2000). *Feeding in paleognathous birds. In: Feeding: Form, Function, and Evolution in Tetrapod Vertebrates (K. Schwenk ed). San Diego: Academic Press, pp. 359–394.*

Tables:

Table 1. Length and width of the different parts of the tongue of the Eurasian teal (*Anas crecca*)

Parts of the oropharyngeal cavity floor			cm
Length of the rostral part of the lower beak that does not occupy by the tongue			0.5 ± 0.12
Tongue	**Length**	**Rostral free part (Till beginning of lingual frenulum)**	2.8 ± 0.33
		Caudal fixed part	1.4 ± 0.23
		Tongue	4.2 ± 0.56
		Lingual nail	0.4 ± 0.02
		Apex	1.4 ± 0.32
		Body	2.4 ± 0.76
		Root	0.4 ± 0.12
	Width	**Lingual nail**	0.6 ± 0.10
		Apex	0.8 ± 0.34
		Body	0.85 ± 0.32
		Root	0.6 ± 0.21
	Thickness	**Lingual nail**	0.2 ± 0.01
		Apex	0.3 ± 0.03
		Body	0.5 ± 0.1
		Root	0.42 ± 0.11
Papillary crest	**Length**		1.4 ± 0.32
Median lingual groove	**Length**		3.2 ± 0.76
Lateral serrated border of the root	**Length**		0.25 ± 0.01
	Width		0.4 ± 0.03
Each half of the dorsal spinated border of the root	**Length**		0.4 ± 0.1
	Width		0.3 ± 0.02

Table 2. Length and width of the different parts of the laryngeal region of the Eurasian teal (*Anas crecca*)

Parts of the laryngeal region			cm
Length of Pharyngeal cavity			1.3 ± 0.23
Papillary (pre-glottic) triangular area			0.4 ± 0.1
Non-papillary glottic elevated area (Laryngeal mound)	**Length**		0.9 ± 0.12
		Rostral part	0.45 ± 0.12
	Width	**Middle part**	0.61 ± 0.24
		Caudal part	0.3 ± 0.11
	Equatorial diameter		2.8 ± 0.54
	Axial diameter		1.52 ± 0.64
Glottis	**Length**		0.5 ± 0.1
	Width		0.2 ± 0.01

Table 3. Average Length and width of the lingual papillae on the different parts of the tongue of the Eurasian teal (*Anas crecca*)

Lingual regions	Papillary type	Average length (µm)	Average width (µm)
Apex	Ridge-like papillae	1.7 ± 0.53	0.28 ± 0.1
	Small pointed filiform papillae	1.4 ± 0.32	0.39 ± 0.12
Body	Rod-like filiform papillae	1.25 ± 0.32	0.26 ± 0.01
	Ventral rod-like filiform papillae	2.13 ± 0.47	0.27 ± 0.01
	Small filiform papillae	0.46 ± 0.1	0.04 ± 0.01
	Large quadrilateral conical papillae	2.5 ± 0.78	0.89 ± 0.34
	Large triangular conical papillae	1.563 ± 0.42	0.51 ± 0.1
	Hair-like filiform papillae	0.31 ± 0.02	0.032 ± 0.01
	Small pointed filiform papillae of the caudal part of the lateral border	0.41 ± 0.01	0.17 ± 0.01

Table 4. Length and width of the papillary border and crest of the tongue of the Eurasian teal (*Anas crecca*)

Papillary type		**Papillary Number**	**Average length (µm)**	**Average width (µm)**
Papillary crest	**Papillae of the dorsal row**	16–18	0.71 ± 0.08	0.2 ± 0.01
	Papillae of ventral row	14–16	0.55 ± 0.06	0.17 ± 0.01
Dorsal spinated border of the root	**Small pointed conical papillae of the dorsal row**	7-8	0.31 ± 0.01	0.05 ± 0.001
	Large triangular pointed conical papillae of the ventral row	6-7	0.45 ± 0.02	0.17 ± 0.02
Lateral serrated border of root	**Triangular papillae**	10–11	0.3 ± 0.02	0.15 ± 0.01
Lateral serrated border of rostral part of the prominence	**Small triangular-pointed**	10-11	0.09 ± 0.01	0.05 ± 0.01

Table 5. Length and width of the papillary border and crest of the laryngeal region of the Eurasian teal (*Anas crecca*)

Papillary type			Papillary Number	Average length (µm)	Average width (µm)
Papillary border of the glottis	**Conical papillae**		10–12	0.25 ± 0.01	0.07 ± 0.001
Diamond-shaped pharyngeal papillae	**7 or 8 transverse rows**	**Conical papillae**	16–18	0.4 ± 0.1	0.23 ± 0.02
			14–16	0.26 ± 0.07	0.09 ± 0.01
			12–14	0.25 ± 0.06	0.06 ± 0.02
			10–8	0.19 ± 0.01	0.05 ± 0.01
			8–6	0.2 ± 0.01	0.04 ± 0.01
			8–6	0.27 ± 0.08	0.03 ± 0.02
			4-6	0.2 ± 0.09	0.03 ± 0.01
	One longitudinal row	**Long, pointed papillae**	5–6	0.64 ± 0.15	0.18 ± 0.02

Figures

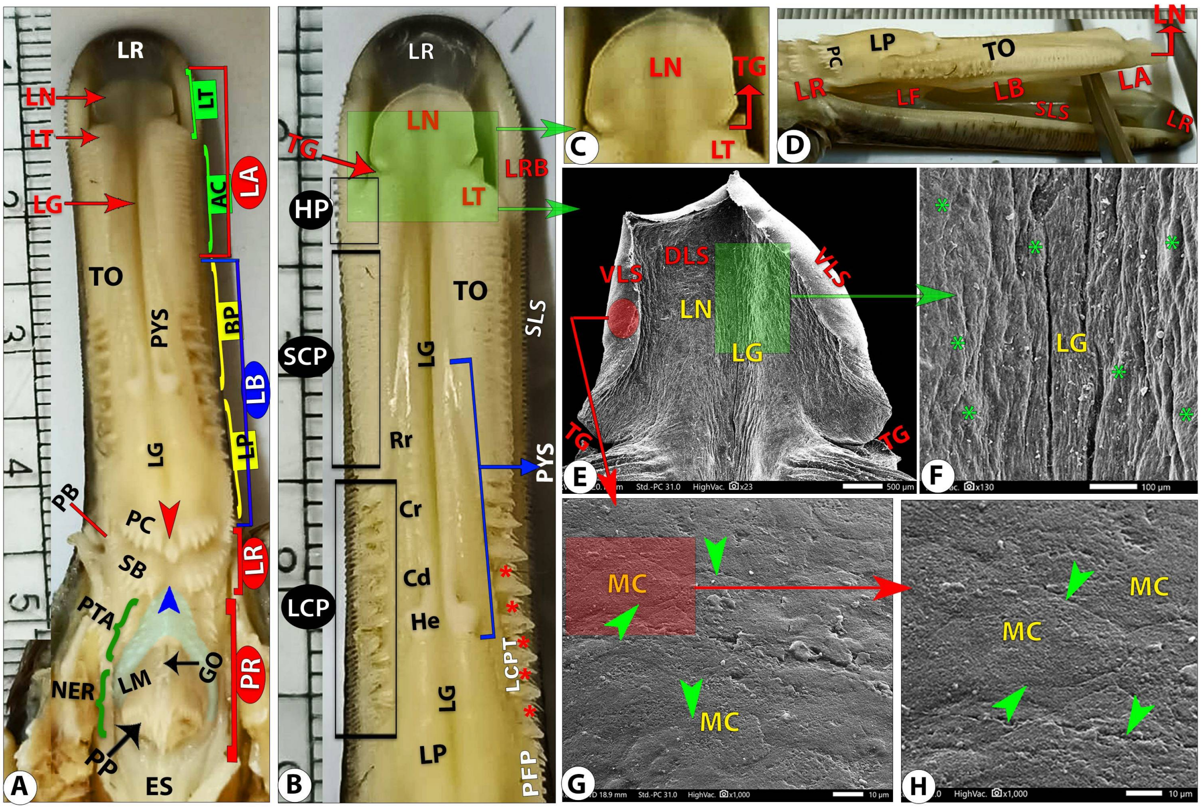

Figure 1. Gross (A-D) and SEM (E-H) images of the floor of the oropharyngeal cavity of *Anas crecca* showing the external serrated surface (SLR) of lateral lower mandibular ramus (LRB), sublingual space (SLS), rostral short smooth space (SDR), lingual frenulum (LF), tongue (TO) with apex (LA) of ridged papillae (HP), tip (LT), nail (LN), transverse groove (TG), body (LB) of lingual comb, small (SCP) and large (SCP) conical papillae had a rostral pyramidal part (BP) and caudal lingual prominence (LP), root (LR) with its papillary crest (PC), large papillae (red arrowhead), serrated border (SB) with median space (blue arrowheads). The pharyngeal region (PR) had papillary triangular (PTA) and non-papillary elevated regions (NER) that had a mound (LM), glottis (GO), and pharyngeal papillae (PP). The medial groove (LG), lingual comb (PYS) had a head (He) and column of caudal (Cd), middle (Cr), and rostral (Rr) parts. The lingual nail (LN) had a dorsal surface (DLS) of numerous small tubercles (green stars) and a ventral surface of numerous micro-cells of different shapes (MC) that were surrounded by micro-grooves (green arrowheads), and Esophagus (ES).

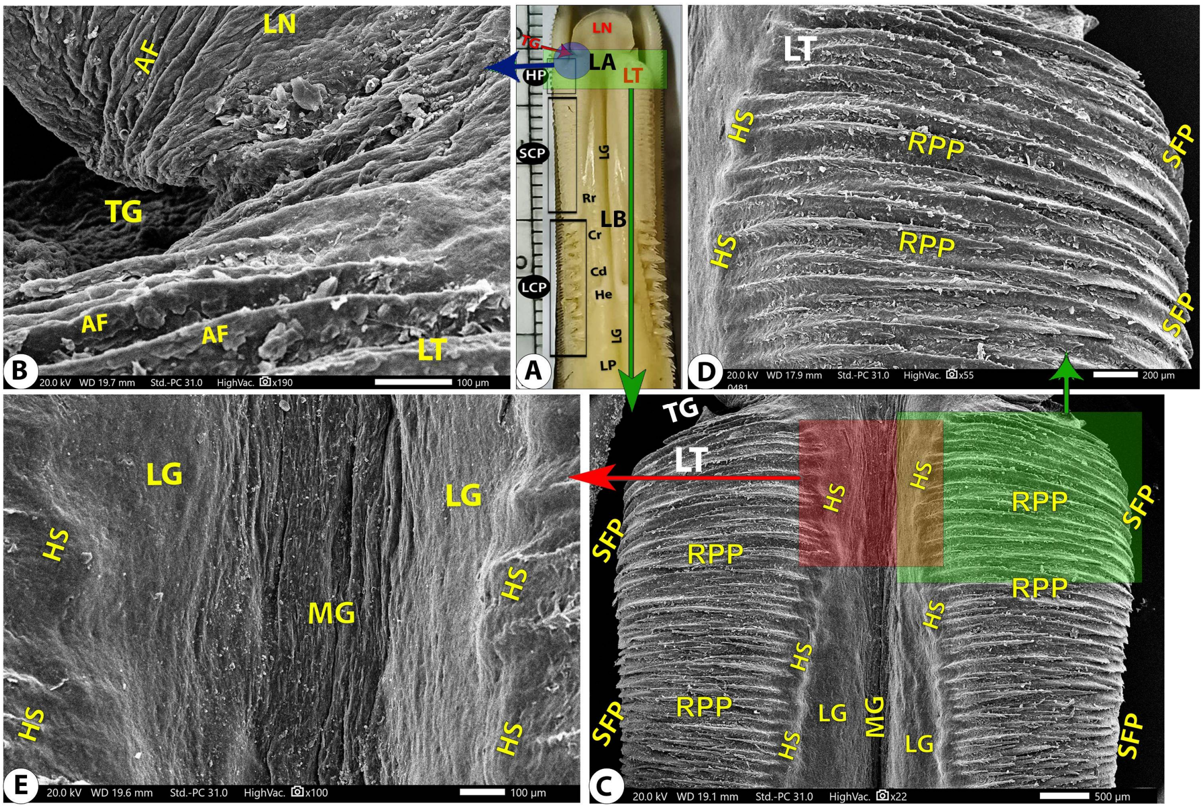

Figure 2. Gross (A) and SEM (B-E) images of the tongue of *Anas crecca* showing the apex (LA), nail (LN), transverse groove (TG), and folds (AF). The tip (LT) carried ridge-like papillae (RPP) of the projected base (HS) and small filiform papillae (SFP). The median groove (LG), deep median groove (MG), and body (LB) carried small (SCP) and large (SCP) conical papillae. The prominence (LP) and the lingual comb (PYS) with its head (He) and column of caudal (Cd), middle (Cr), and rostral (Rr) parts.

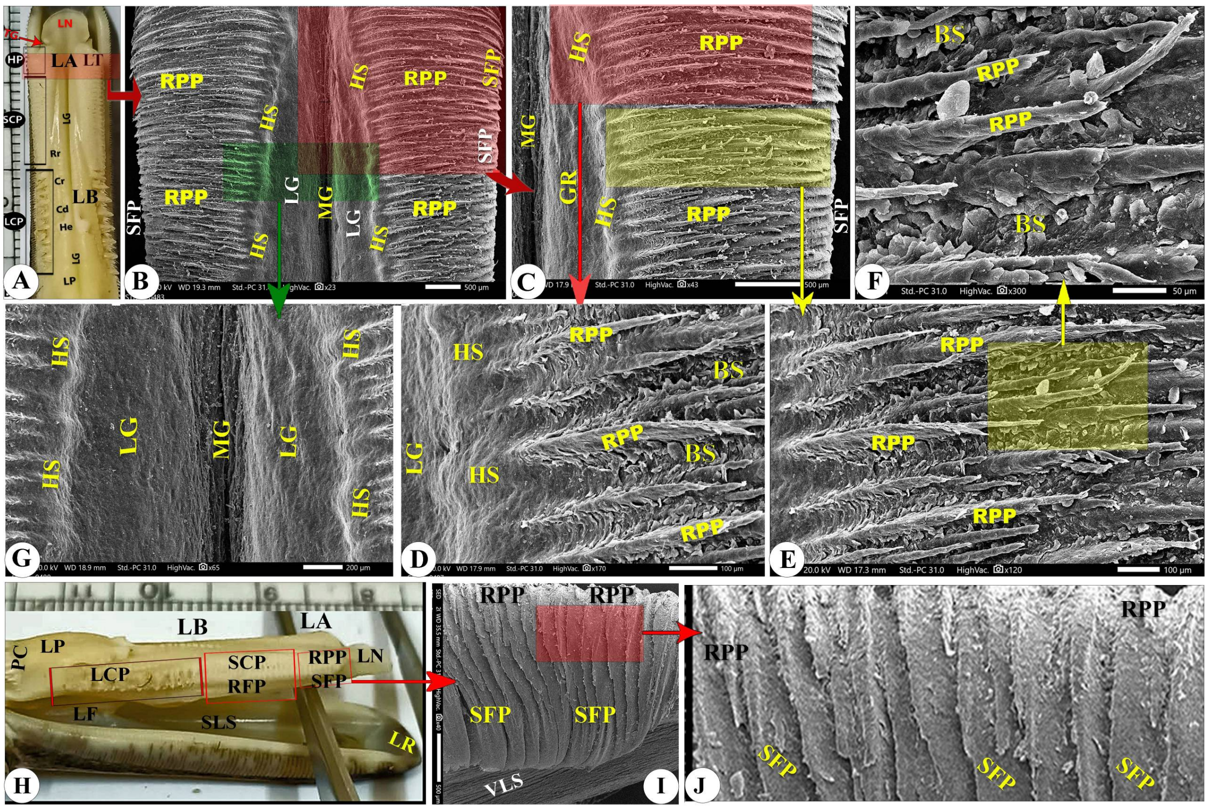

Figure 3. Gross (A and H) of the lower mandibular beak and SEM (B-G and I-J) images of the apex (LA) of *Anas crecca* show that the nail (LN), transverse groove (TG), tip (LT), ridge-like papillae (RPP) of the projected base (HS), small filiform papillae (SFP), scales (BS), lingual groove (LG), deep groove (MG), body (LB), papillary crest (PC), small (SCP) and large (SCP) conical papillae, small filiform papillae (SFP), lingual prominence (LP), ventral lingual surface (VLS), lingual frenulum (LF), sublingual space (SLS), the external serrated surface (SLR) of the lateral lower mandibular ramus (LRB), and dorsal beak surface (SDR). The lingual comb (PYS) had a head (He) and column of caudal (Cd), middle (Cr), and rostral (Rr) parts.

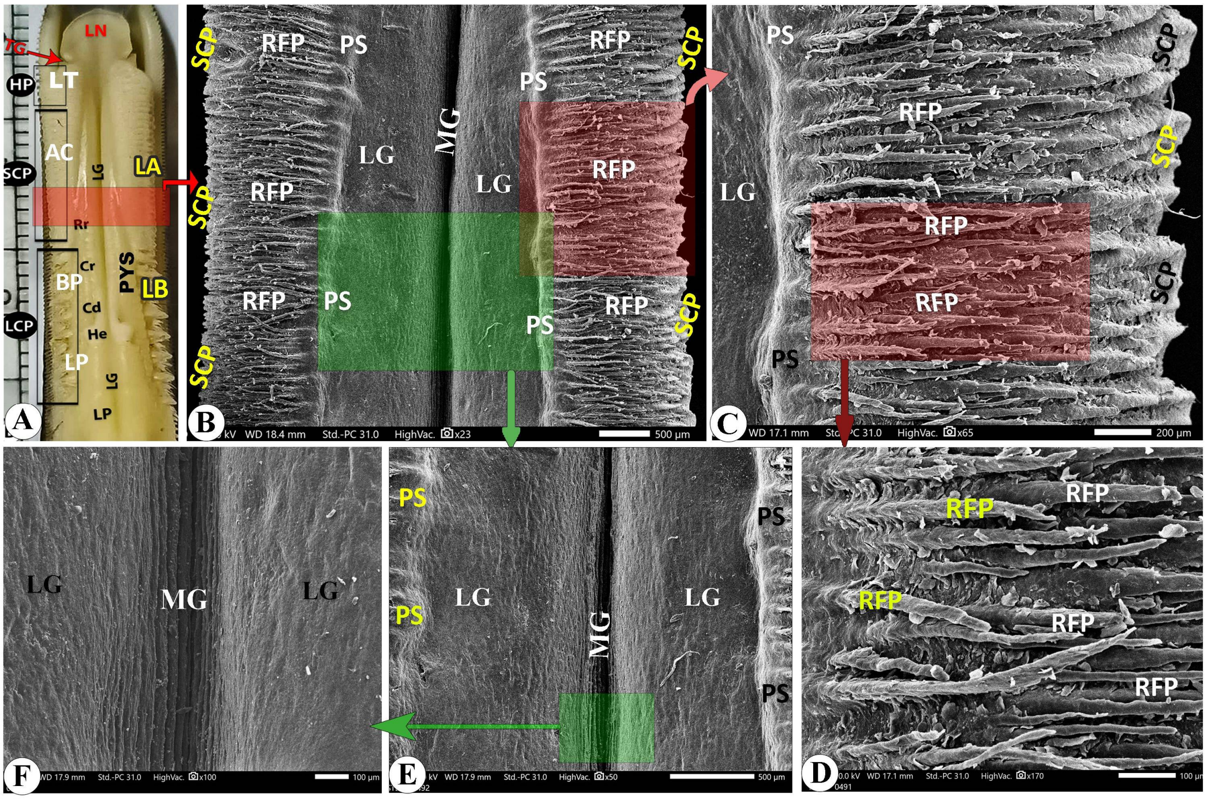

Figure 4. Gross (A) of the tongue and SEM of the lingual body (B-F) images of *Anas crecca* showing apex (LA), tip (LT), nail (LN), transverse groove (TG), numerous ridge-like papillae (HP), body (LB), a rostral pyramidal part (BP) with rod-like filiform papillae (RFP), a projected base (PS), and small conical papillae (SCP), while the lingual prominence (LP) with large conical papillae (LCP). The lingual groove (LG), deep groove (MG), and lingual comb (PYS) had heads (He) and columns of caudal (Cd), middle (Cr), and rostral (Rr) parts.

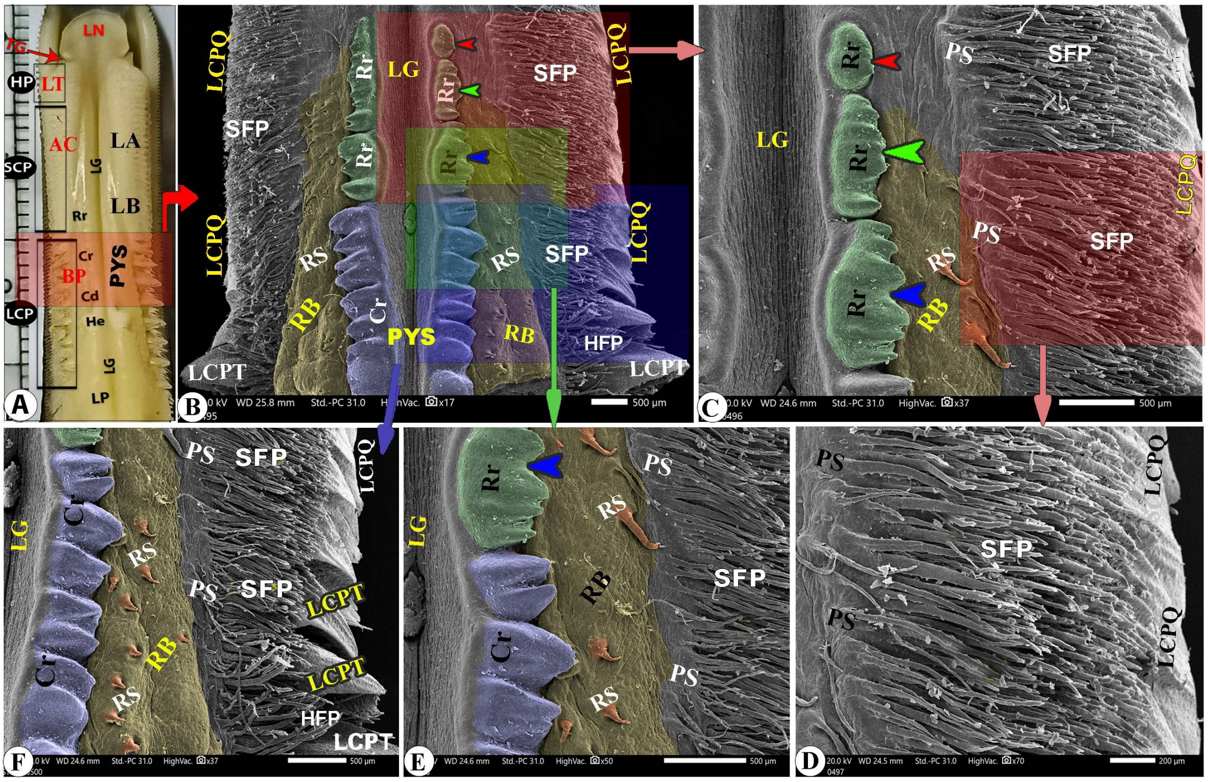

Figure 5. Gross (A) of the tongue and SEM of the lingual body (B-F) images of *Anas crecca* show the apex (LA), tip (LT), nail (LN), transverse groove (TG), ridge-like papillae (HP), body (LB), a rostral pyramidal part (BP) with small conical papillae (SCP) and small filiform papillae (SFP) with its base (PS), large quadrilateral conical papillae (LCPQ), randomly distributed spines (RS), and round tubercles (RB) at its rostral part, and large triangular conical papillae (LCPT) with hair-like filiform papillae (HFP). The prominence (LP), groove (LG), and the lingual comb (PYS) with its head (He) and column of caudal part (Cd), middle part (Cr), and rostral (Rr) part are three portions (blue, green, and red arrowheads).

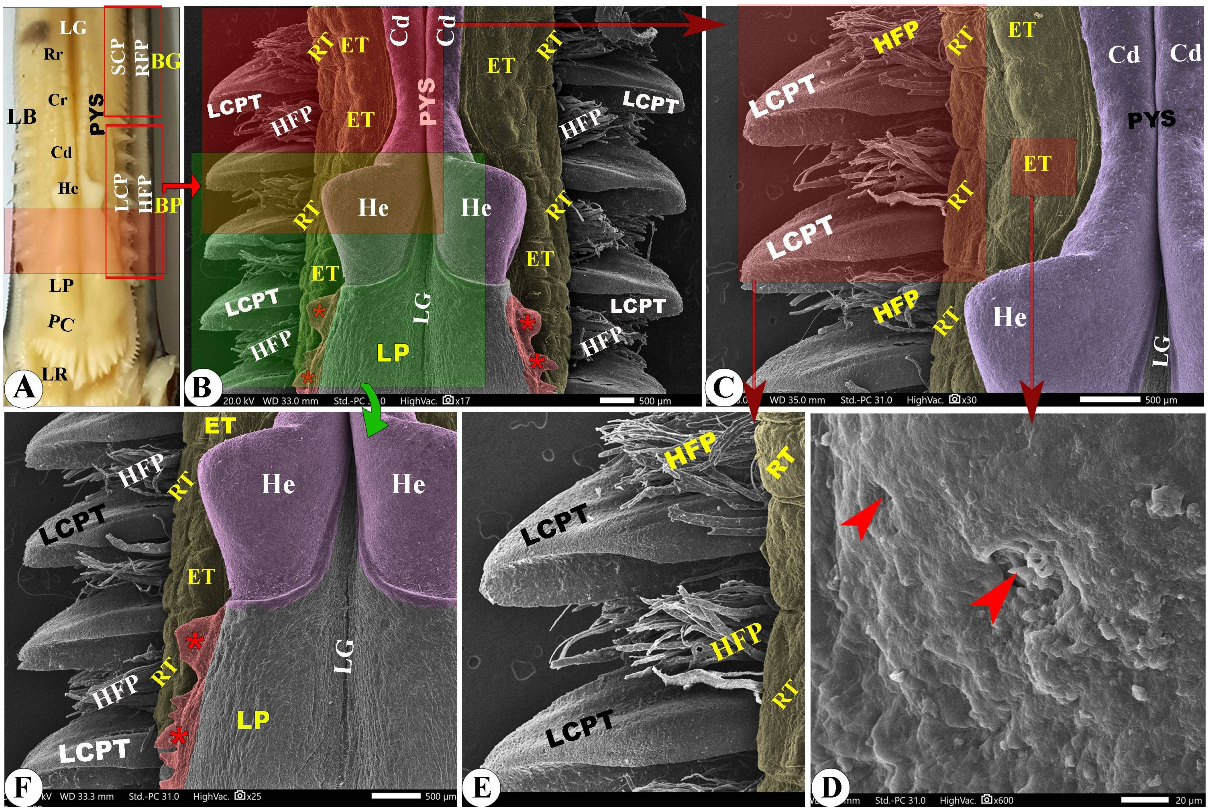

Figure 6. Gross (A) of the tongue and SEM of the lingual body (B-F) images of *Anas crecca* showing the body (LB), rostral pyramidal part (BP) with large triangular conical papillae (LCPT), and hair-like filiform papillae (HFP). The prominence (LP) with its serrated rostral portion (red stars) had large triangular conical papillae (LCPT) with hair-like filiform papillae (HFP), round tubercles (RT), elevated tubercles (ET), salivary gland openings (red arrowheads) at its posterior part, the groove (LG), papillary crest (PC), and root (LR), and the and the lingual comb (PYS) with its head (He) and column of caudal (Cd), middle (Cr), and rostral (Rr) parts.

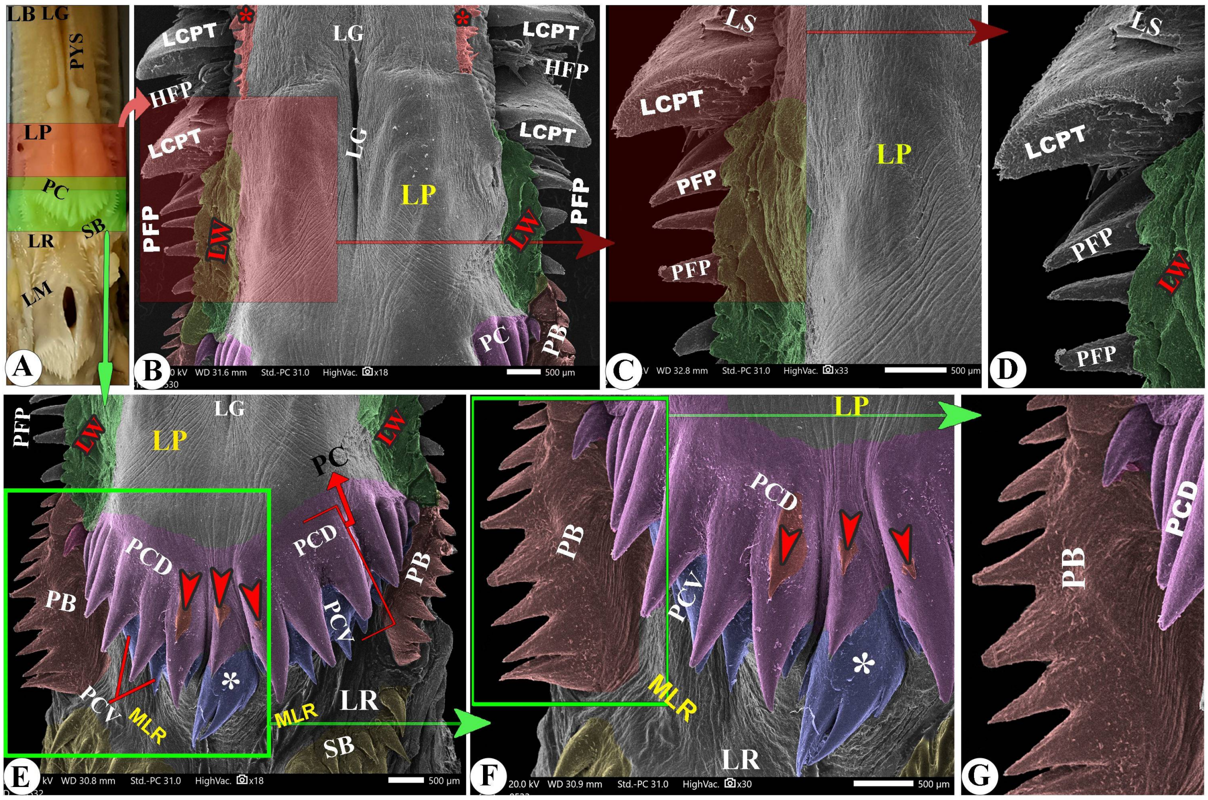

Figure 7. Gross (A) and SEM (B-F) images of the lingual body of *Anas crecca* showing the body (LB), lingual groove (LG), lingual comb (PYS), lingual prominence (LP), papillary crest (PC) with its dorsal (PCD) that had small accessory papillae (red arrowheads) and ventral papillary row (PCV) with its median large ones (white star), large triangular conical papillae (LCPT) with hair-like filiform papillae (HFP), pointed filiform papillae (PFP) and wing (LW). The root (LR) has a median smooth part (MLR), a serrated border (SB), and a pointed lateral border (PB).

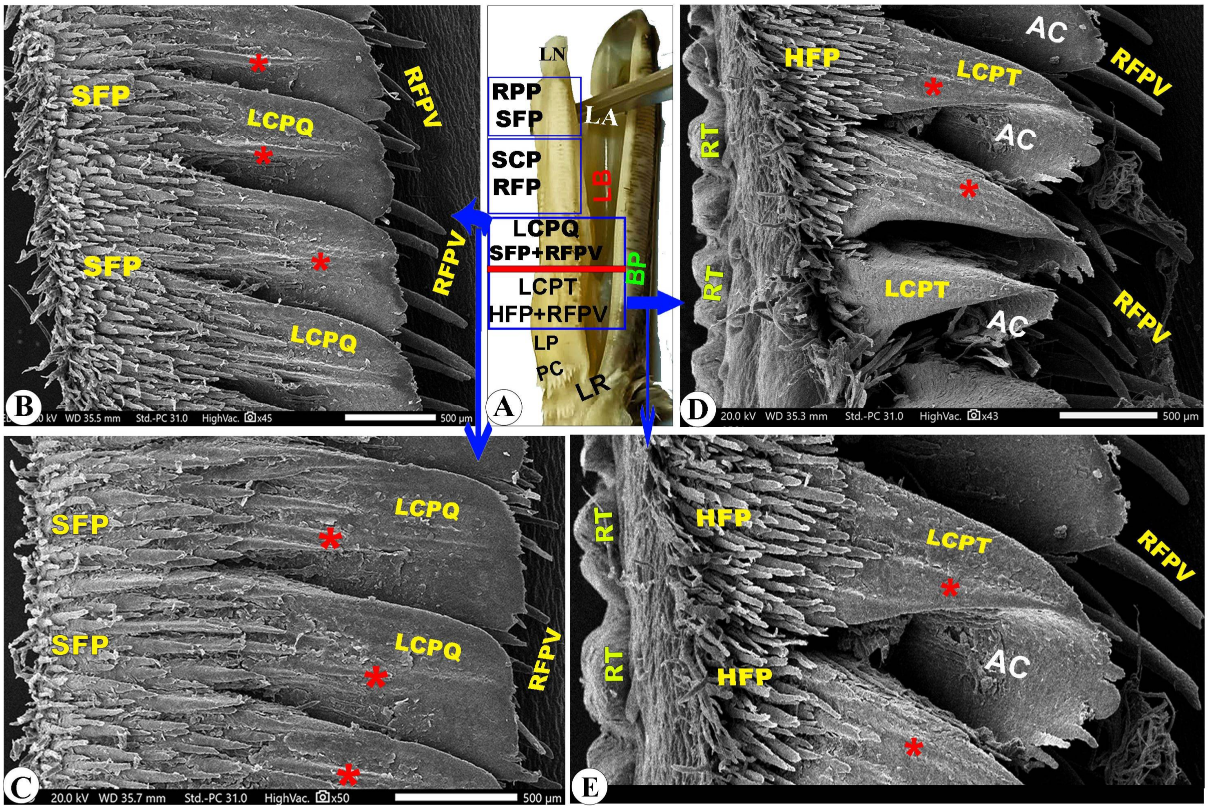

Figure 8. Gross (A) and SEM (B-E) images of the lateral lingual surface of *Anas crecca* showing the apex (LA), nail (LN), ridge-like papillae (RPP), and small filiform papillae (SFP). The body (LB) had a rostral pyramidal part (BP) with small conical papillae (SCP) and rod-like filiform papillae (RFP), while the prominence (LP) had ventral rod-like filiform papillae (RFPV), large quadrilateral (LCPQ) and triangular (LCPT) conical papillae, hair-like processes (HFP) with a median ridge (red stars), accessory fan-like structure (AC), and round tubercles (RT). The lingual root (LR) has a papillary crest (PC).

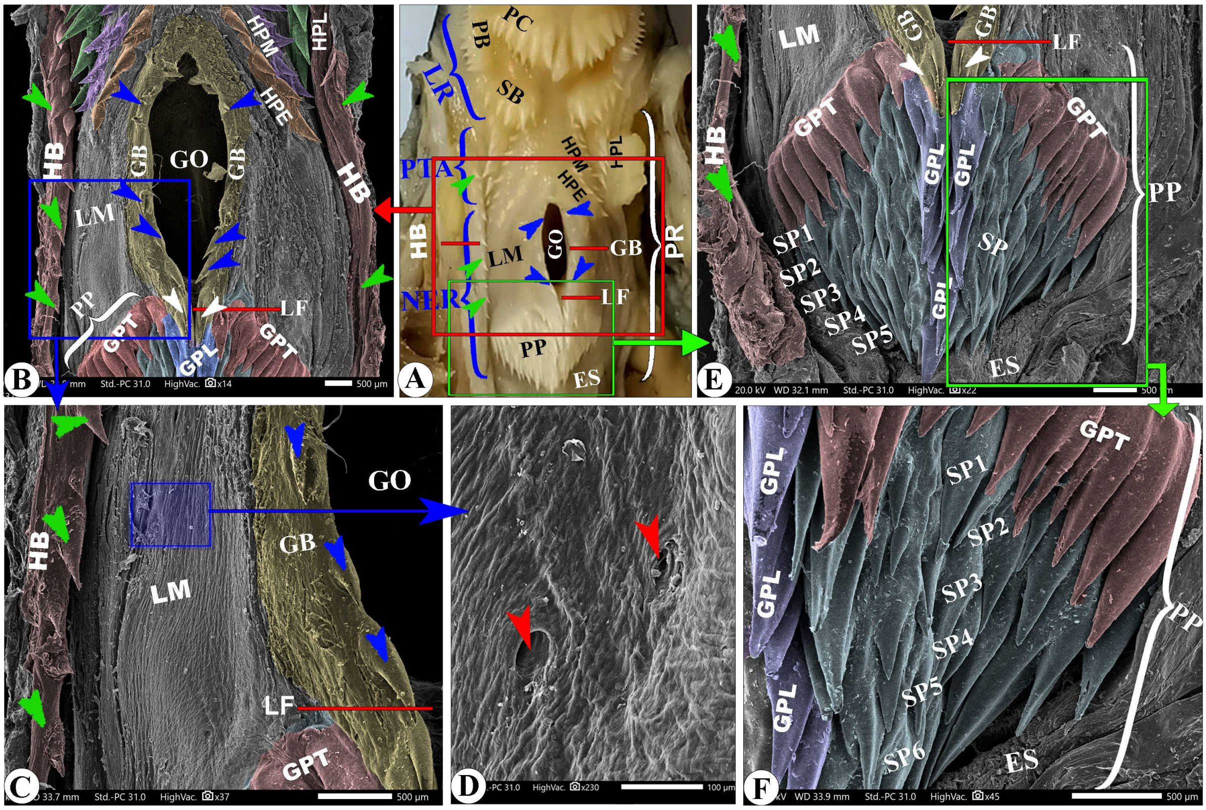

Figure 9. Gross (A) and SEM (B-F) images of the tongue of *Anas crecca* showing the body (LB), groove (LG), comb (PYS), prominence (LP), and the papillary crest (PC) with its large median papillae (red arrowheads). The root (LR) has a spinated border (SB) with its rostral (SBR) and posterior papillary row (SBR), a narrow passage (blue arrowheads), and a processed border (PB). P The pharyngeal region (PR) had a papillary triangular part (PTA) with their papillae (HP) that were arranged in three papillary rows: lateral (HPL) with accessory papillae (red star), middle (HPM) with accessory papillae (green star), and medial (HPE) row with papillary scales (HS), while the non-papillary elevated part (NER) had a laryngeal mound (LM), glottic opening (GO), pharyngeal papillae (PP), and esophagus (ES).

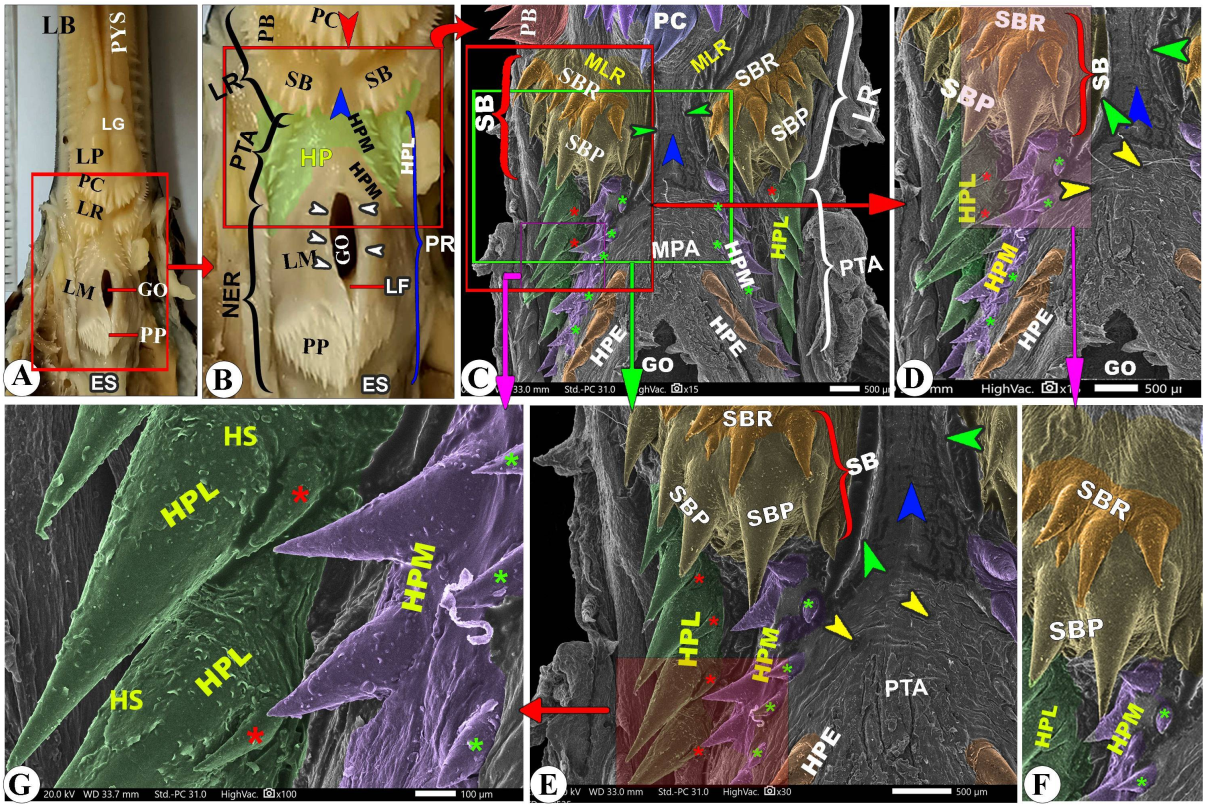

Figure 10. Gross (A) and SEM (B-F) images of the laryngeal entrance of *Anas crecca* showing the root (LR), papillary crest (PC), spinated border (SB), narrow passage (blue arrowheads), and processed border (PB). Pharyngeal region (PR) had papillary triangular part (PTA) with their papillae (HP) that were arranged in three papillary rows: lateral (HPL), middle (HPM), and medial (HPE) rows with papillary scales (HS), while the non-papillary elevated part (NER) had their laryngeal mound (LM) with laryngeal gland openings (red arrowheads) and was surrounded by longitudinal laryngeal border (HB) with their spines (green arrowheads), glottic opening (GO) with its papillary border (GB), spines (blue arrowheads), and laryngeal cleft (LF). Pharyngeal papillae (PP) are arranged in seven rows: the rostral slightly oblique transverse row (GPT), the median longitudinal row (GPL), the six transverse rows (SP 1-6), and the esophagus (ES).